



Observation of muonic Dalitz decays of χ_b mesons and precise spectroscopy of hidden-beauty states

LHCb collaboration[†]

Abstract

The decays of the $\chi_{b1}(1P)$, $\chi_{b2}(1P)$, $\chi_{b1}(2P)$ and $\chi_{b2}(2P)$ mesons into the $\Upsilon(1S)\mu^+\mu^-$ final state are observed with a high significance using proton-proton collision data collected with the LHCb detector and corresponding to an integrated luminosity of 9 fb^{-1} . The newly observed decays together with the $\Upsilon(2S) \rightarrow \Upsilon(1S)\pi^+\pi^-$ and $\Upsilon(3S) \rightarrow \Upsilon(2S)\pi^+\pi^-$ decay modes are used for precision measurements of the mass and mass splittings for the hidden-beauty states.

Published in [Journal of High Energy Physics 10 \(2024\) 122](#)

© 2024 CERN for the benefit of the LHCb collaboration. [CC BY 4.0 licence](#).

[†]Authors are listed at the end of this paper.

1 Introduction

Measurements of the properties of quarkonium states provide a test of QCD potential models [1–4]. While the charmonium system is precisely mapped out [5, 6], the experimental knowledge of hidden beauty states is more limited. In Ref. [7] it was shown that the clean experimental signature of χ_c decaying to the $J/\psi\mu^+\mu^-$ final state, referred to as muonic Dalitz decays hereafter, provides a new method to precisely measure properties of charmonia. In this paper, the corresponding measurements in the hidden beauty system are made. The first observation of the muonic Dalitz decays of the $\chi_{b1}(1P)$, $\chi_{b2}(1P)$, $\chi_{b1}(2P)$, and $\chi_{b2}(2P)$ mesons to the $\Upsilon(1S)$ state and measurement of the masses of these states is reported. These results have very different systematic uncertainties compared to those obtained from the measurement of the photon energy in $\Upsilon(2S)$ or $\Upsilon(3S)$ transitions to the $\chi_{b1,2}(1P)$ or $\chi_{b1,2}(2P)$ states [8–12]. Since these decay modes only involve muons, greater precision and better control of systematics can be achieved compared to studies with radiative modes involving converted photons [13]. In addition, the $\Upsilon(3S) \rightarrow (\Upsilon(2S) \rightarrow \mu^+\mu^-)\pi^+\pi^-$ and $\Upsilon(2S) \rightarrow (\Upsilon(1S) \rightarrow \mu^+\mu^-)\pi^+\pi^-$ decay modes are used to make precise measurements of the Υ meson masses and mass splittings.¹ As well as providing valuable input to QCD potential models, better knowledge of the Υ meson masses will improve the precision of electroweak measurements such as that of the W boson mass, where hidden beauty decays provide a standard method for detector calibration [14].

This analysis uses LHCb data collected in proton-proton (pp) collisions between 2011 and 2018. The data from 2011 and 2012, collectively referred to as Run 1, were collected at centre-of-mass energies of 7 and 8 TeV and correspond to integrated luminosities of 1 fb^{-1} and 2 fb^{-1} , respectively. The rest of the data, referred to as Run 2, were collected between 2015 and 2018 at a centre-of-mass energy of 13 TeV and correspond to an integrated luminosity of 6 fb^{-1} .

2 Detector and simulation

The LHCb detector [15, 16] is a single-arm forward spectrometer that covers the pseudorapidity range $2 < \eta < 5$, designed for the study of particles containing b or c quarks. It includes a high-precision tracking system consisting of a silicon-strip vertex detector surrounding the pp interaction region, a large-area silicon-strip detector located upstream of a dipole magnet with a bending power of approximately 4 Tm, and three stations of silicon-strip detectors and straw drift tubes placed downstream of the magnet. The tracking system provides a measurement of the momentum, p , of charged particles with a relative uncertainty that varies from 0.5% at low momentum to 1.0% at 200 GeV/c. Large samples of $J/\psi \rightarrow \mu^+\mu^-$ and $B^+ \rightarrow J/\psi K^+$ decays, collected concurrently with the dataset used in this analysis, are used to calibrate the momentum scale of the spectrometer [17]. The relative uncertainty achieved on the momentum scale is 3×10^{-4} . Charged hadrons are distinguished using information from two ring-imaging Cherenkov (RICH) detectors. In addition, photons, electrons, and hadrons are identified by a calorimeter system consisting of scintillating-pad and preshower detectors, an elec-

¹In this paper, the symbol Υ denotes the $\Upsilon(1S)$, $\Upsilon(2S)$ and $\Upsilon(3S)$ states together, and the symbol χ_b stands for the $\chi_{b1}(1P)$, $\chi_{b2}(1P)$, $\chi_{b1}(2P)$ and $\chi_{b2}(2P)$ states.

tromagnetic and a hadronic calorimeter. Muons are identified by a system composed of alternating layers of iron and multiwire proportional chambers [18, 19].

The online event selection is performed by a trigger, which consists of a hardware system followed by a two-level software stage [20, 21]. At the hardware trigger stage, events are required to have either a muon track with high transverse momentum or a dimuon candidate with a high value for the product of the p_T of the muons. For the Run 2 dataset, the alignment and calibration of the detector is performed in near real-time such that the results are used in the software trigger [22]. The same alignment and calibration information is propagated to the offline reconstruction, ensuring consistent information between the trigger and offline software. The first level of the software trigger performs a partial event reconstruction and requires events to have a pair of well-identified oppositely charged muons with a reconstructed mass larger than $2.7 \text{ GeV}/c^2$. The second level performs a full event reconstruction. Events are retained for further processing if they contain a high-mass dimuon candidate.

This analysis makes limited use of simulation. The main input needed from simulation is the resolution model for the mass distribution of the signal decays. This is obtained using the RAPIDSIM fast-simulation package [23]. This has been tuned using the LHCb full simulation, implemented with the GEANT4 toolkit [24, 25] as described in Ref. [26]. In both simulation frameworks, decays of hadronic particles are described by EVTGEN [27], in which final-state radiation is generated using PHOTOS [28, 29]. The $\Upsilon(2S) \rightarrow \Upsilon(1S)\pi^+\pi^-$ decay follows the model described in Refs. [30–32], the $\Upsilon(3S) \rightarrow \Upsilon(2S)\pi^+\pi^-$ decay uses a phase-space distribution, and the Dalitz decays are based on the approach described in Ref. [33]. The p_T spectrum for hidden beauty mesons is taken from the LHCb studies of Υ production presented in Refs. [34–38].

3 $\Upsilon \rightarrow \mu^+\mu^-$ selection and mass fits

The selection starts from a pair of oppositely charged muons, selected by the trigger as an $\Upsilon \rightarrow \mu^+\mu^-$ candidate. Combinatorial background is efficiently rejected by a requirement on the output of a boosted decision tree classifier [39, 40], referred to as BDT hereafter, implemented in the TMVA toolkit [41, 42]. The BDT classifier is trained on a small fraction of the data using the *sPlot* technique [43], with the dimuon mass as the discriminating variable, to distinguish signal and background. As inputs, the classifier uses seventeen variables related to the decay kinematics, track quality [44–47], vertex quality and particle identification information [19, 48]. A loose requirement on the BDT output reduces the combinatorial background by a factor of four, whilst only removing 1% of the signal.

The dimuon mass distribution obtained after the BDT requirement is shown in Fig. 1. A fit is made to this distribution to extract the mass parameters. In this fit the $\Upsilon(1S) \rightarrow \mu^+\mu^-$, $\Upsilon(2S) \rightarrow \mu^+\mu^-$ and $\Upsilon(3S) \rightarrow \mu^+\mu^-$ signals are described by modified Gaussian functions with power-law tails on both sides of the distribution [49, 50]. The tail parameters of the modified Gaussian functions are shared between the three signal peaks, and allowed to vary in the fit, while their widths are constrained to scale linearly with the dimuon mass [34–37]. A third-order polynomial is used to describe the background. Due to the very large data sample a binned extended maximum-likelihood fit is used. The bin width, of $1 \text{ MeV}/c^2$, is chosen to be sufficiently narrow so that it does not affect

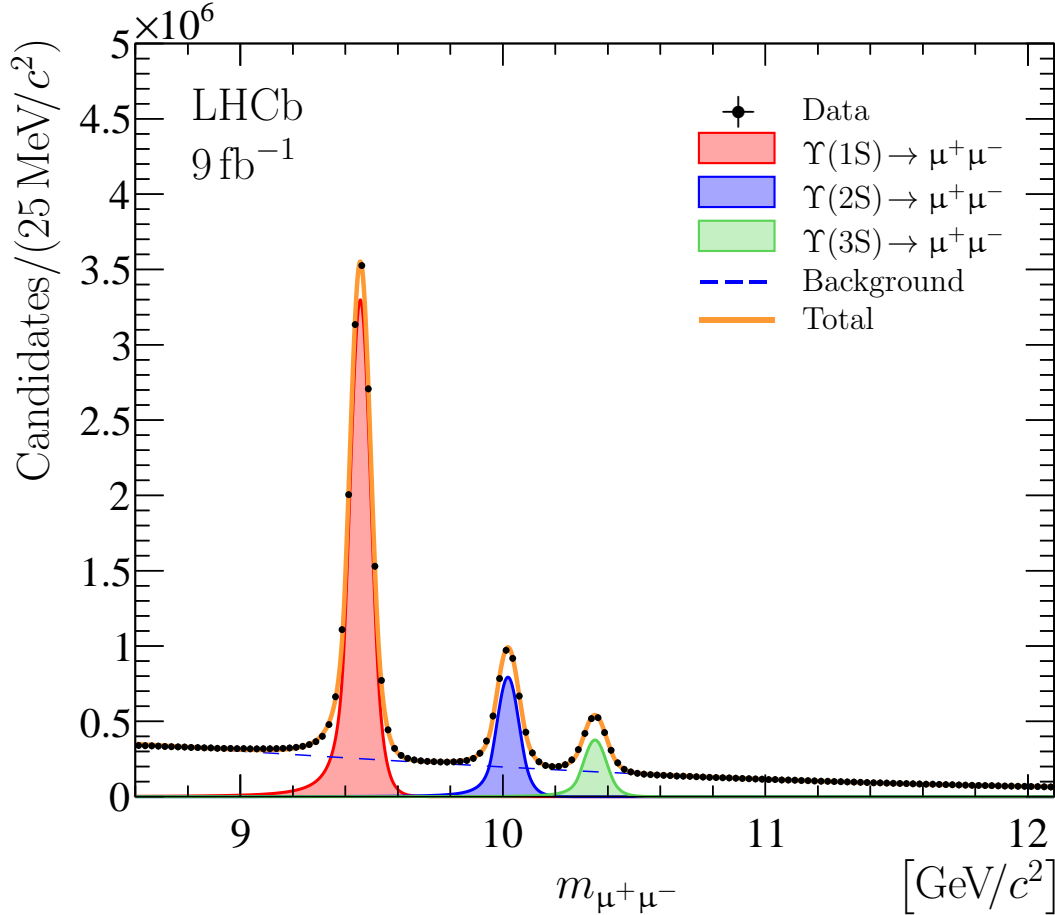


Figure 1: Dimuon mass spectrum after the BDT requirement. The result of the fit described in the text is overlaid.

the determination of the Υ masses. For the considered fit range the efficiency is found to be a smooth and slowly varying function of the dimuon mass, not affecting the mass measurements. The measured masses and mass differences are corrected for the effect of QED radiative processes using simulation. The correction for the $\Upsilon(1S)$ mass is large, $3.27 \text{ MeV}/c^2$. It largely cancels in the mass splittings, resulting in residual corrections of 0.29 and $0.14 \text{ MeV}/c^2$ for the $m_{\Upsilon(2S)} - m_{\Upsilon(1S)}$ and $m_{\Upsilon(3S)} - m_{\Upsilon(2S)}$ differences, respectively.

Table 1: Parameters of interest, yields N_{Υ} , masses and mass differences, from the fit to the dimuon mass spectra. The uncertainties are statistical only.

Parameter		Value
$N_{\Upsilon(1S)}$	$[10^3]$	$14\,609.3 \pm 6.7$
$N_{\Upsilon(2S)}$	$[10^3]$	$3\,729.1 \pm 3.2$
$N_{\Upsilon(3S)}$	$[10^3]$	$1\,827.9 \pm 2.3$
$m_{\Upsilon(1S)}$	$[\text{MeV}/c^2]$	$9\,460.37 \pm 0.01$
$m_{\Upsilon(2S)} - m_{\Upsilon(1S)}$	$[\text{MeV}/c^2]$	562.71 ± 0.04
$m_{\Upsilon(3S)} - m_{\Upsilon(2S)}$	$[\text{MeV}/c^2]$	331.77 ± 0.07

Table 2: Systematic uncertainties on the measurement of the $\Upsilon(1S)$ mass and mass differences from the analysis of the dimuon mass spectrum.

Source of systematic	Uncertainty [MeV/ c^2]		
	$m_{\Upsilon(1S)}$	$m_{\Upsilon(2S)} - m_{\Upsilon(1S)}$	$m_{\Upsilon(3S)} - m_{\Upsilon(2S)}$
Momentum scale	2.8	0.17	0.10
Energy loss correction	0.02	—	—
Radiative corrections	0.13	0.03	0.03
Fit model	0.35	0.10	0.02
Sum in quadrature	2.85	0.20	0.10

The large yields for the $\Upsilon \rightarrow \mu^+ \mu^-$ modes and the low-background level, lead to a small statistical uncertainty on the mass parameters, given in Table 1. The dominant systematic uncertainty on the $\Upsilon(1S)$ mass, $2.8 \text{ MeV}/c^2$, is due to the knowledge of the momentum scale [17]. In the mass differences, this uncertainty largely cancels, giving an uncertainty of $0.17 \text{ MeV}/c^2$ for the $m_{\Upsilon(2S)} - m_{\Upsilon(1S)}$ and $0.10 \text{ MeV}/c^2$ for the $m_{\Upsilon(3S)} - m_{\Upsilon(2S)}$ splitting. An additional uncertainty arises from the size of the energy-loss correction applied in the track fit [51]. Varying the detector material within its 10% uncertainty and rerunning the track fit results in a $20 \text{ keV}/c^2$ uncertainty for two-body decay modes. Further uncertainties arise from the knowledge of the radiative corrections and the assumed fit model. The systematic uncertainty from the modelling of the former is estimated by running PHOTOS with different settings [17, 52] and largely cancels in the mass differences. The uncertainty on the latter is evaluated using alternative fit models for the background, which include convex decreasing polynomials of order two, three, or four; generic polynomials of the second and fourth order; and a product of an exponential function and a first-order polynomial function. As an alternative signal shape, a modified Gaussian function with tail parameters constrained to values obtained in previous LHCb analyses [34–38, 53–55] is considered. The total systematic uncertainties for the mass and mass difference measurements are summarised in Table 2.

4 $\Upsilon(2S) \rightarrow \Upsilon(1S)\pi^+\pi^-$ and $\Upsilon(3S) \rightarrow \Upsilon(2S)\pi^+\pi^-$ selection and mass fits

The $\Upsilon \rightarrow \mu^+ \mu^-$ candidates with mass in the regions $9.343 < m_{\mu^+\mu^-} < 9.556 \text{ GeV}/c^2$ and $9.899 < m_{\mu^+\mu^-} < 10.124 \text{ GeV}/c^2$ are considered as $\Upsilon(1S) \rightarrow \mu^+ \mu^-$ and $\Upsilon(2S) \rightarrow \mu^+ \mu^-$ candidates, respectively. Each mass region contains 95% of the corresponding decays, according to the fit described in Sec. 3. To form $\Upsilon(2S) \rightarrow \Upsilon(1S)\pi^+\pi^-$ and $\Upsilon(3S) \rightarrow \Upsilon(2S)\pi^+\pi^-$ candidates, selected $\Upsilon(1S) \rightarrow \mu^+ \mu^-$ and $\Upsilon(2S) \rightarrow \mu^+ \mu^-$ candidates are combined with pairs of oppositely charged particles identified as pions by the RICH system [48, 56]. Combinatorial background is reduced by requiring the scalar sum of the p_T of the pions to be larger than $400 \text{ MeV}/c$. To further suppress background, a parameter

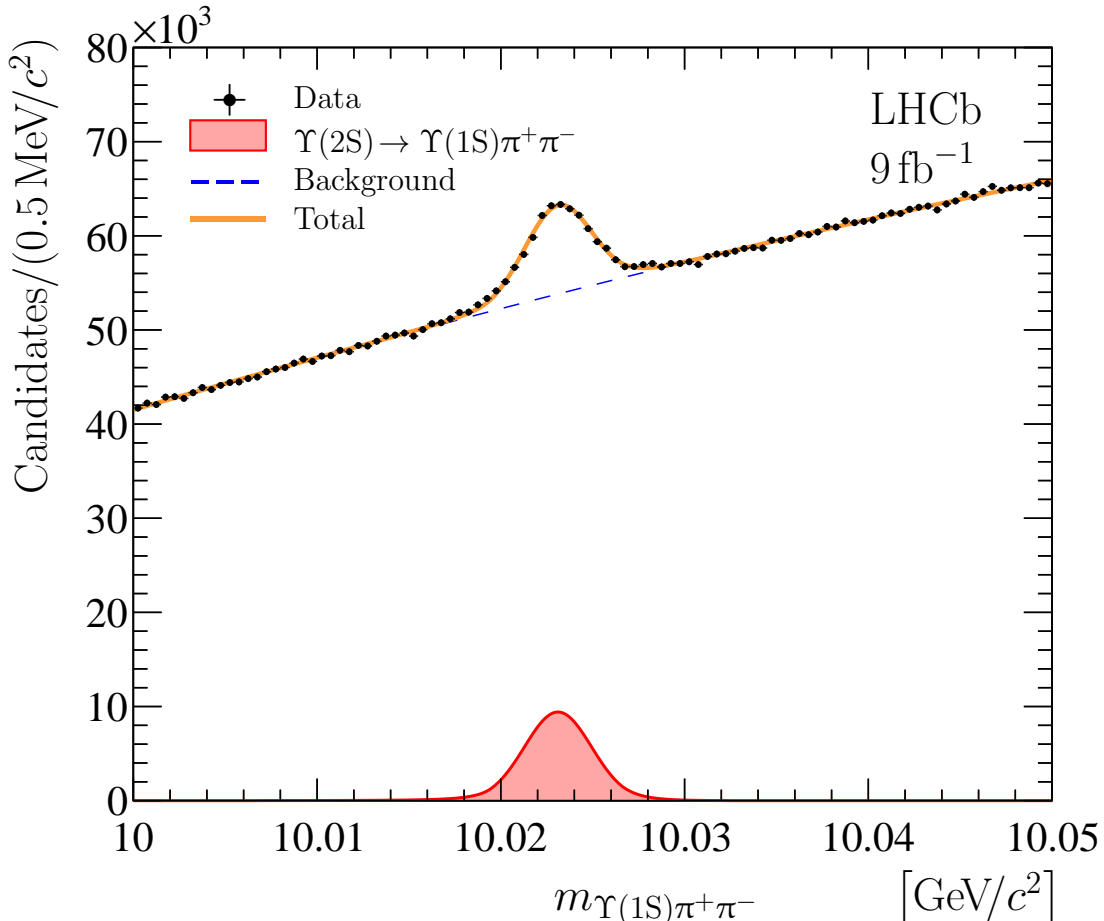


Figure 2: Mass spectrum of $\Upsilon(1S)\pi^+\pi^-$ candidates with a constraint on the $\Upsilon(1S)$ mass applied. The result of the fit described in the text is overlaid.

$x_{\pi^+\pi^-}$ is introduced as

$$x_{\pi^+\pi^-} \equiv \frac{m_{\pi^+\pi^-} - 2m_\pi}{m_{\Upsilon\pi^+\pi^-} - m_\Upsilon - 2m_\pi}, \quad (1)$$

where $m_{\pi^+\pi^-}$, m_Υ and $m_{\Upsilon\pi^+\pi^-}$ stand for the masses of the $\pi^+\pi^-$, $\mu^+\mu^-$ and $\Upsilon\pi^+\pi^-$ systems, and m_π is the known mass of the charged pion [57]. Candidates are required to satisfy a loose requirement, $x_{\pi^+\pi^-} > 0.2$. A kinematic fit [58] is made to the selected candidates, constraining the dimuon mass to the known $\Upsilon(1S)$ or $\Upsilon(2S)$ mass [57], indicated in Table 7, as appropriate, and requiring the candidate to be consistent with coming from a primary pp collision vertex. The χ^2 per degree of freedom of this fit, $\chi^2_{\text{fit}}/\text{ndf}$, is required to be less than five.

The $\Upsilon(1S)\pi^+\pi^-$ and $\Upsilon(2S)\pi^+\pi^-$ mass spectra are shown in Figs. 2 and 3, respectively. A fit to the $\Upsilon(1S)\pi^+\pi^-$ mass spectrum is performed using a function consisting of signal and combinatorial background components. The signal component is described using the modified Gaussian function described in Sec. 3, with all parameters fixed from the simulation apart from the peak location and a scale factor s_f for the width, which allows for differences between data and simulation [59–63]. The background component is modelled by an increasing third-order polynomial function. An extended binned maximum-likelihood fit is used with the bin width of 100 keV/c^2 chosen to be sufficiently narrow so that it does not affect the $\Upsilon(2S)$ mass determination. The fit result is overlaid in Fig. 2

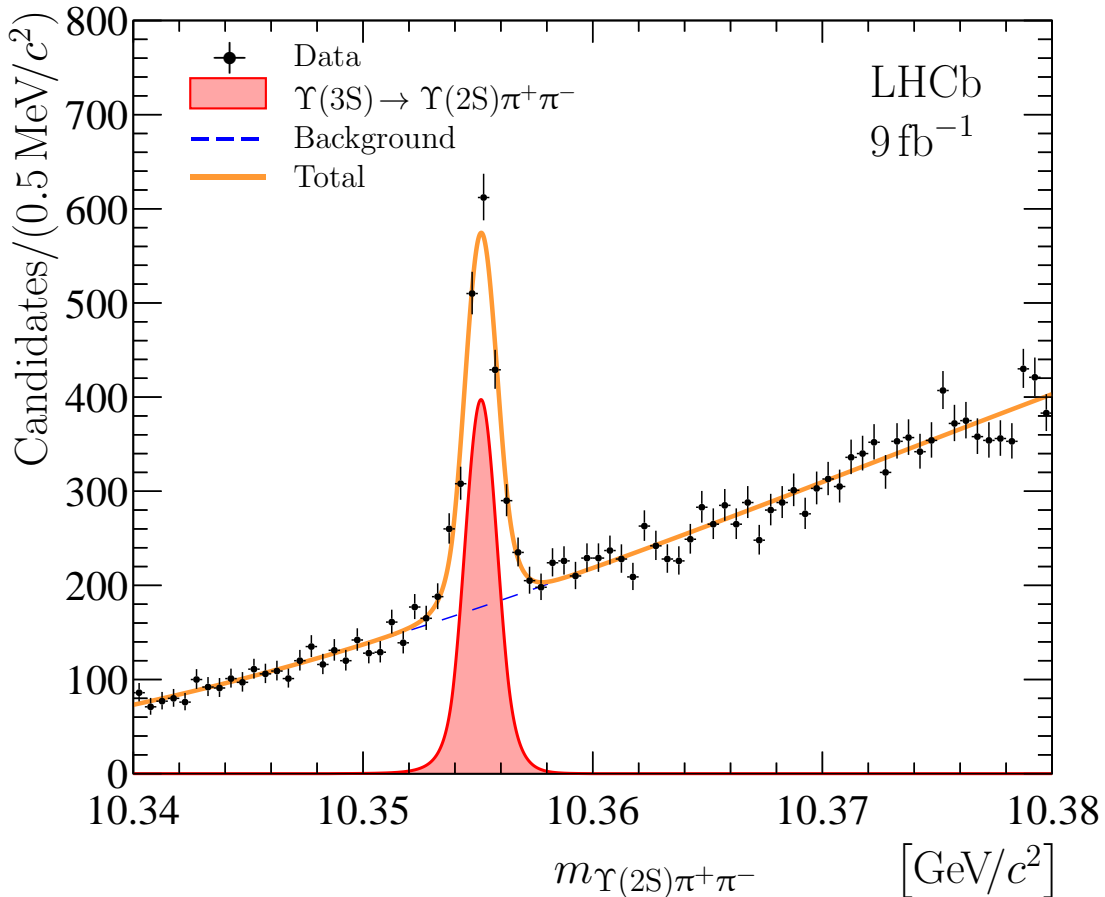


Figure 3: Mass spectrum of $\Upsilon(2S)\pi^+\pi^-$ candidates with a constraint on the $\Upsilon(2S)$ mass applied. The result of the fit described in the text is overlaid.

and the results for the parameters of interest are listed in Table 3. The mass results in Table 3 include a correction for QED radiation. The value of $s_f = 1.015 \pm 0.012$ is found to be consistent with unity.

A similar signal model, obtained from simulation, is used to fit the $\Upsilon(2S)\pi^+\pi^-$ mass spectrum. In this case the background component is described by an increasing convex third-degree polynomial function. For this fit, the resolution scale factor is Gaussian-constrained to the value obtained for the $\Upsilon(2S) \rightarrow \Upsilon(1S)\pi^+\pi^-$ signal above. The result of an extended unbinned maximum-likelihood fit is overlaid in Fig. 3 and the results for the parameters of interest are listed in Table 3. The combined resolution scale factor determined from the fits to the $\Upsilon(2S) \rightarrow \Upsilon(1S)\pi^+\pi^-$ and the $\Upsilon(3S) \rightarrow \Upsilon(2S)\pi^+\pi^-$ signals is

$$s_f = 1.012 \pm 0.012. \quad (2)$$

Since the $\Upsilon(1S) \rightarrow \mu^+\mu^-$ and $\Upsilon(2S) \rightarrow \mu^+\mu^-$ candidates are constrained to their known masses [57], the residual corrections to the measured $\Upsilon(2S)$ and $\Upsilon(3S)$ masses and their differences are small. Furthermore, the corrections numerically cancel for the mass splitting determined to be

$$m_{\Upsilon(3S)} - m_{\Upsilon(2S)} = 332.03 \pm 0.04 \text{ MeV}/c^2, \quad (3)$$

where the uncertainty is statistical only.

Table 3: Values for the parameters of interest, yields N and masses, from the fits to the $\Upsilon(1S)\pi^+\pi^-$ and $\Upsilon(2S)\pi^+\pi^-$ mass spectra. Uncertainties are statistical only.

Parameter		Value
$N_{\Upsilon(2S)\rightarrow\Upsilon(1S)\pi^+\pi^-}$	$[10^3]$	88.55 ± 1.05
$N_{\Upsilon(3S)\rightarrow\Upsilon(2S)\pi^+\pi^-}$	$[10^3]$	1.46 ± 0.05
$m_{\Upsilon(2S)}$	$[\text{MeV}/c^2]$	$10\,023.25 \pm 0.03$
$m_{\Upsilon(3S)}$	$[\text{MeV}/c^2]$	$10\,355.28 \pm 0.03$

Table 4: Systematic uncertainties on the measurement of the $\Upsilon(2S)$ and $\Upsilon(3S)$ mass parameters, and the mass difference from the analysis of the $\Upsilon(2S)\rightarrow\Upsilon(1S)\pi^+\pi^-$ and $\Upsilon(3S)\rightarrow\Upsilon(2S)\pi^+\pi^-$ decays.

Source of systematic	Uncertainty $[\text{keV}/c^2]$		
	$m_{\Upsilon(2S)}$	$m_{\Upsilon(3S)}$	$m_{\Upsilon(3S)} - m_{\Upsilon(2S)}$
Momentum scale	120	33	87
Energy loss correction	20	20	—
Radiative corrections	3	2	1
Fit model	8	2	6
Sum in quadrature	122	39	89

The statistical uncertainty for the $\Upsilon(2S)$ and $\Upsilon(3S)$ mass difference from Eq. (3) is slightly smaller than that in Table 1 despite the much lower signal yield and larger background level. This reflects the better mass resolution for the $\Upsilon(2S)\rightarrow\Upsilon(1S)\pi^+\pi^-$ and $\Upsilon(3S)\rightarrow\Upsilon(2S)\pi^+\pi^-$ signals. For the mass and mass difference, the same sources of systematic uncertainty as described in Sec. 3 are considered. The dominant uncertainty is due to the knowledge of the momentum scale. The uncertainty related to the signal and background parameterisation is estimated using a set of alternative fit models. The systematic uncertainties for the mass measurements from analysis of the $\Upsilon(1S)\pi^+\pi^-$ and $\Upsilon(2S)\pi^+\pi^-$ mass spectra are summarised in Table 4. The $\Upsilon(2S)$ and $\Upsilon(3S)$ mass measurements are made with the $\Upsilon(1S)$ and $\Upsilon(2S)$ masses constrained to their known values [57]. The uncertainties in these values are propagated as an external systematic uncertainty on the mass measurements and discussed in Sec. 6. The background-subtracted $x_{\pi^+\pi^-}$ distributions for the $\Upsilon(2S)\rightarrow\Upsilon(1S)\pi^+\pi^-$ and $\Upsilon(3S)\rightarrow\Upsilon(2S)\pi^+\pi^-$ decays are found to be similar to simulation and previous measurements by the ARGUS [64] and CLEO [65] collaborations.

5 $\chi_b \rightarrow \Upsilon(1S)\mu^+\mu^-$ selection and mass fits

Candidate $\chi_b \rightarrow \Upsilon(1S)\mu^+\mu^-$ decays are formed by combining the selected $\Upsilon(1S)\rightarrow\mu^+\mu^-$ candidates with oppositely charged particles, identified as muons. In this case, the requirements on muon identification [19, 48] and track quality [47] are sufficient

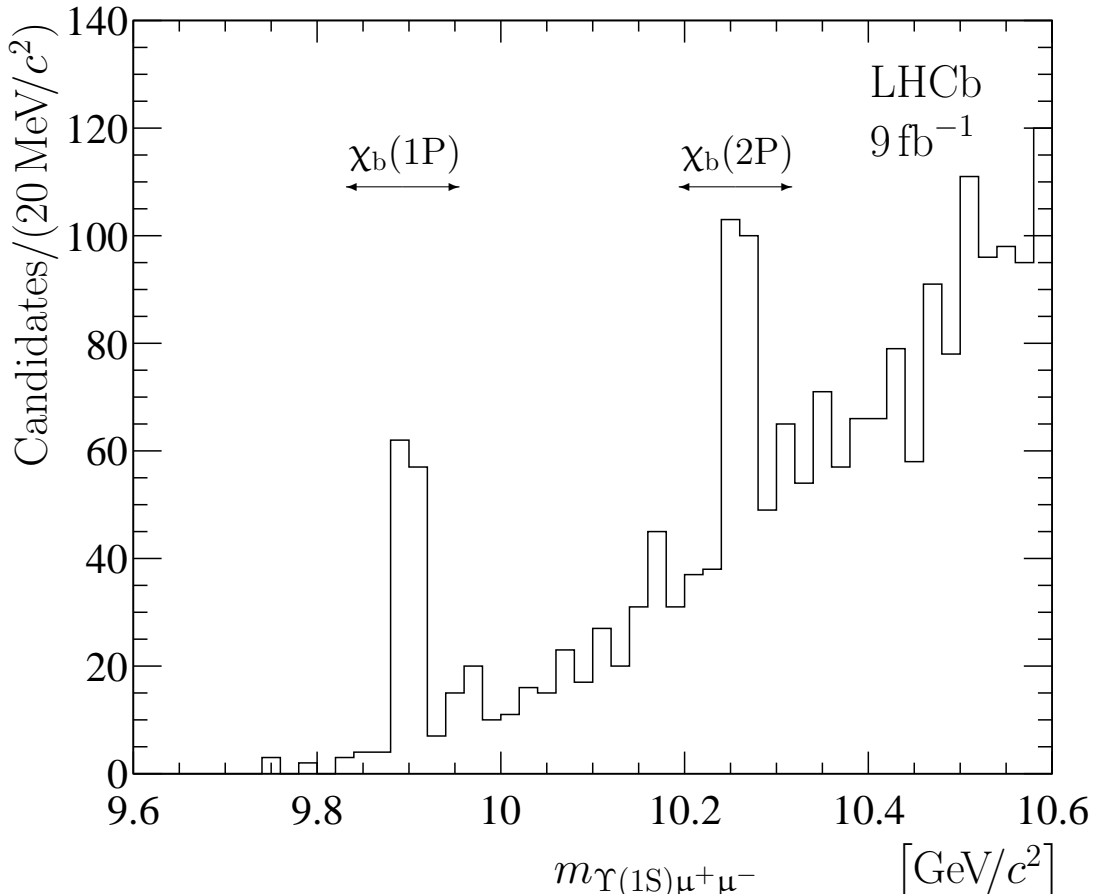


Figure 4: Mass spectrum of $\Upsilon(1S)\mu^+\mu^-$ candidates with a constraint on the $\Upsilon(1S)$ mass applied.

to reduce the combinatorial background, mainly originating from pions that decay in flight. The only additional requirement needed is on the kinematic fit quality $\chi_{\text{fit}}^2/\text{ndf} < 5$. The $\Upsilon(1S)\mu^+\mu^-$ mass spectrum, for combinations that meet the full set of selection criteria, is shown in Fig. 4.

Extended unbinned maximum-likelihood fits to the $\Upsilon(1S)\mu^+\mu^-$ mass spectrum are made separately for the $\chi_b(1P)$ and $\chi_b(2P)$ regions, defined as $9.84 < m_{\Upsilon(1S)\mu^+\mu^-} < 9.96 \text{ GeV}/c^2$ and $10.20 < m_{\Upsilon(1S)\mu^+\mu^-} < 10.32 \text{ GeV}/c^2$, respectively. For each region the fit function consists of three components: two signal components, describing the axial-vector and tensor χ_b states, modelled by the modified Gaussian functions with shape parameters fixed from simulation, and a background component taken as a positive second-order polynomial function. The natural widths of the χ_b states are assumed to be small, as predicted in Refs. [2, 4, 66–68], and are neglected. In these fits, the width parameters of the Gaussian functions are scaled with a factor s_f , that is Gaussian-constrained from Eq. (2). The results of the fits are overlaid in Figs. 5 and 6 and summarised in Table 5. The statistical significance is calculated for each the four observed $\chi_b \rightarrow \Upsilon(1S)\mu^+\mu^-$ decays using Wilks' theorem [69] and also listed in Table 5. The mass splittings for the $\chi_b(1P)$ and $\chi_b(2P)$ states are found to be

$$\delta m_{\chi_b(1P)} \equiv m_{\chi_{b2}(1P)} - m_{\chi_{b1}(1P)} = 19.4 \pm 0.4 \text{ MeV}/c^2, \quad (4a)$$

$$\delta m_{\chi_b(2P)} \equiv m_{\chi_{b2}(2P)} - m_{\chi_{b1}(2P)} = 15.7 \pm 1.0 \text{ MeV}/c^2, \quad (4b)$$

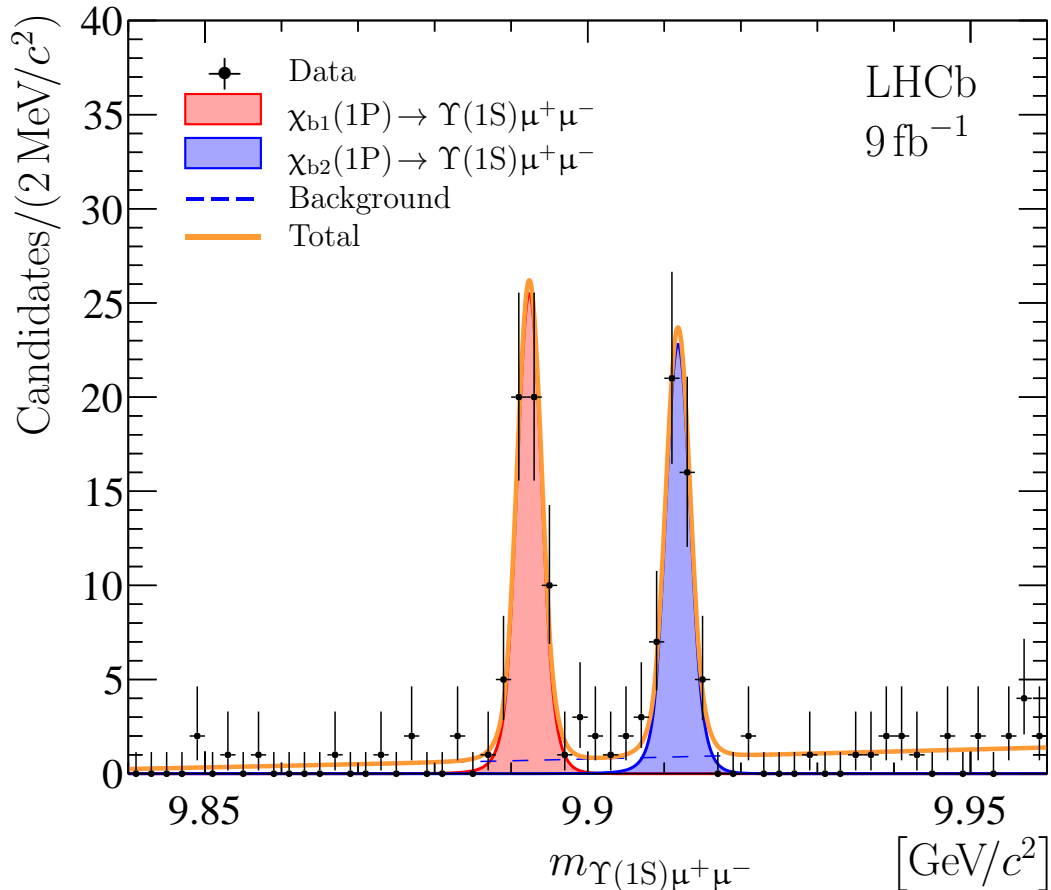


Figure 5: Mass spectrum of $\Upsilon(1S)\mu^+\mu^-$ candidates in the $\chi_b(1P)$ region with a constraint on the $\Upsilon(1S)$ mass applied. The result of the fit described in the text is overlaid.

Table 5: The parameters of interest, yields N and masses, from the fits to the $\Upsilon(1S)\mu^+\mu^-$ mass spectrum. The uncertainties are statistical only. The last column shows the statistical significance of the signals in units of standard deviations.

Parameter	Value	\mathcal{S}
$N_{\chi_{b1}(1P)\rightarrow\Upsilon(1S)\mu^+\mu^-}$	53.6 ± 7.7	12.4
$N_{\chi_{b2}(1P)\rightarrow\Upsilon(1S)\mu^+\mu^-}$	47.9 ± 7.4	11.5
$N_{\chi_{b1}(2P)\rightarrow\Upsilon(1S)\mu^+\mu^-}$	51.1 ± 10.4	6.5
$N_{\chi_{b2}(2P)\rightarrow\Upsilon(1S)\mu^+\mu^-}$	59.3 ± 10.4	7.2
$m_{\chi_{b1}(1P)}$ [MeV/ c^2]	9892.50 ± 0.26	
$m_{\chi_{b2}(1P)}$ [MeV/ c^2]	9911.92 ± 0.29	
$m_{\chi_{b1}(2P)}$ [MeV/ c^2]	10253.97 ± 0.75	
$m_{\chi_{b2}(2P)}$ [MeV/ c^2]	10269.67 ± 0.67	

where the uncertainties are statistical only.

Systematic uncertainties for the masses of the χ_b states and mass splittings are evaluated using the same techniques described in Sec. 4 for the $\Upsilon(2S)$ and $\Upsilon(3S)$ masses and $\Upsilon(3S) - \Upsilon(2S)$ mass difference. The uncertainties are summarised in Table 6. Again,

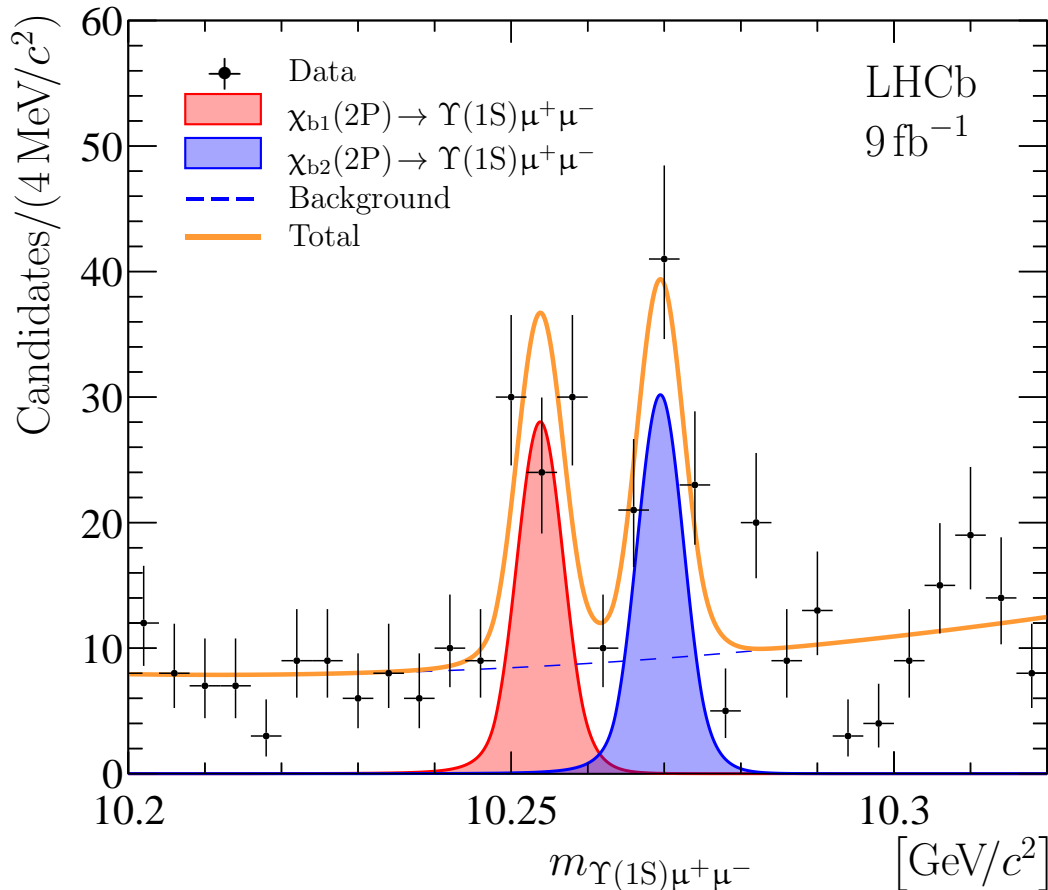


Figure 6: Mass spectrum of $\Upsilon(1S)\mu^+\mu^-$ candidates in the $\chi_b(2P)$ region with a constraint on the $\Upsilon(1S)$ mass applied. The result of the fit described in the text is overlaid.

the dominant uncertainty is related to knowledge of the momentum scale, and largely cancels for the mass splittings. For the systematic uncertainty associated with the fit model, a set of alternative signal models are probed. To test alternative parameterisations of the background, first-order polynomial functions are used, as well as a product of a three-body phase-space function [70] and the first- and second-order polynomials. An additional systematic uncertainty is related to the assumption of the negligible natural width for the χ_b states. To estimate the associated uncertainty, signal shapes are parameterised as relativistic Breit–Wigner functions convolved with the detector resolution, and a series of fits are performed scanning the natural widths from 50 to 250 keV, covering the range of theoretical expectations [2, 4, 66–68]. The maximal deviations from the results of the baseline fits are taken as the associated systematic uncertainty. The mass measurements in Table 5 are made with the $\Upsilon(1S)$ mass constrained to the known value [57]. The uncertainty in this value is propagated as an external systematic uncertainty on the mass measurements. The statistical significance for each χ_b state is recalculated for each alternative fit model, and the minimal values of 12.4, 11.2, 6.3 and 7.0 standard deviations are taken as the significance of the $\chi_{b1}(1P)$, $\chi_{b2}(1P)$, $\chi_{b1}(2P)$ and $\chi_{b2}(2P)$ states accounting for the systematic uncertainties.

Table 6: Systematic uncertainties on the measurement of the χ_b masses and mass differences.

Source of systematic	Uncertainty [keV/c ²]					
	$m_{\chi_{b1}(1P)}$	$m_{\chi_{b2}(1P)}$	$m_{\chi_{b1}(2P)}$	$m_{\chi_{b2}(2P)}$	$\delta m_{\chi_b(1P)}$	$\delta m_{\chi_b(2P)}$
Momentum scale	99	106	214	218	7	4
Energy loss correction	20	20	20	20	—	—
Radiative corrections	7	8	13	13	1	—
Fit model	4	3	4	2	6	2
Natural width	—	—	10	10	—	—
Sum in quadrature	101	109	215	219	9	4

6 Results and discussion

A large sample of $\Upsilon \rightarrow \mu^+ \mu^-$ decays is used to measure the masses and mass differences of the Υ states. While the absolute mass measurements have a large systematic uncertainty, the mass differences are measured much more precisely

$$m_{\Upsilon(1S)} = 9\,460.37 \pm 0.01 \pm 2.85 \text{ MeV}/c^2, \quad (5a)$$

$$m_{\Upsilon(2S)} - m_{\Upsilon(1S)} = 562.71 \pm 0.04 \pm 0.20 \text{ MeV}/c^2, \quad (5a)$$

$$m_{\Upsilon(3S)} - m_{\Upsilon(2S)} = 331.77 \pm 0.07 \pm 0.10 \text{ MeV}/c^2, \quad (5b)$$

where the first uncertainty is statistical and the second systematic.

Using $\Upsilon(2S) \rightarrow \Upsilon(1S)\pi^+\pi^-$ decays, where the $\Upsilon(1S)$ mass is constrained [57], a precise measurement of the $\Upsilon(2S)$ mass is made,

$$m_{\Upsilon(2S)} = 10\,023.25 \pm 0.03 \pm 0.12 \pm 0.09 \text{ MeV}/c^2, \quad (6)$$

where the first uncertainty is statistical, the second systematic and the third from the knowledge of the $\Upsilon(1S)$ mass [57]. The uncertainty due to the knowledge of the $\Upsilon(1S)$ mass [57] largely cancels in the mass difference

$$m_{\Upsilon(2S)} - m_{\Upsilon(1S)} = 562.85 \pm 0.03 \pm 0.12 \pm 0.01 \text{ MeV}/c^2. \quad (7)$$

This value agrees with the one obtained with $\Upsilon \rightarrow \mu^+ \mu^-$ decays, Eq. (5a), and they are combined in Appendix A.

Using $\Upsilon(3S) \rightarrow \Upsilon(2S)\pi^+\pi^-$ decays, where the $\Upsilon(2S)$ mass is constrained [57], a precise measurement of the $\Upsilon(3S)$ mass is made,

$$m_{\Upsilon(3S)} = 10\,355.28 \pm 0.03 \pm 0.04 \pm 0.48 \text{ MeV}/c^2, \quad (8)$$

where the first uncertainty is statistical, the second is systematic and the third is from the knowledge of the $\Upsilon(2S)$ mass [57]. The uncertainty due to the knowledge of the $\Upsilon(2S)$ mass largely cancels in the mass difference

$$m_{\Upsilon(3S)} - m_{\Upsilon(2S)} = 331.88 \pm 0.03 \pm 0.04 \pm 0.02 \text{ MeV}/c^2. \quad (9)$$

Table 7: Current knowledge of Υ masses and mass splittings.

Parameter		PDG'22 [71]	PDG'24 [57]
$m_{\Upsilon(1S)}$	[MeV/ c^2]	$9\,460.30 \pm 0.26$	$9\,460.4 \pm 0.1$
$m_{\Upsilon(2S)}$	[MeV/ c^2]	$10\,023.26 \pm 0.31$	$10\,023.4 \pm 0.5$
$m_{\Upsilon(3S)}$	[MeV/ c^2]	$10\,355.2 \pm 0.5$	$10\,355.1 \pm 0.5$
$m_{\Upsilon(3S)} - m_{\Upsilon(2S)}$	[MeV/ c^2]	331.50 ± 0.13	331.50 ± 0.13

Table 8: The Υ mass splittings measured by the BaBar collaboration [72]. These results are not considered in any edition of the PDG.

Parameter	Value
$m_{\Upsilon(2S)} - m_{\Upsilon(1S)}$ [MeV/ c^2]	$562.170 \pm 0.007 \pm 0.088$
$m_{\Upsilon(3S)} - m_{\Upsilon(1S)}$ [MeV/ c^2]	$893.813 \pm 0.015 \pm 0.107$

This is in agreement with the value obtained with $\Upsilon \rightarrow \mu^+ \mu^-$ decays, Eq. (5b), and the two measurements are combined in Appendix A. The dependence on the external knowledge of the $\Upsilon(2S)$ mass is also removed by using the $\Upsilon(2S)$ mass given in Eq. (6) instead of the value given in the 2024 edition of the particle data group averages (PDG'24) [57]. Assuming the uncertainties from the momentum scale and energy loss correction are fully correlated, it gives

$$m_{\Upsilon(3S)} = 10\,355.13 \pm 0.04 \pm 0.15 \pm 0.09 \text{ MeV}/c^2, \quad (10)$$

where the last uncertainty is due to the knowledge of the $\Upsilon(1S)$ mass [57].

These measurements can be compared to the current experimental knowledge of the Υ masses summarised in Tables 7 and 8. Direct measurements of the Υ masses come from studies made in the 1980s by the MD-1 collaboration at the VEPP-4 storage rings [73–75], the CUSB collaboration at the CESR accelerator [76], and a joint study by the ARGUS and Crystal Ball collaborations at the DORIS II collider [77]. Recently, these data have been reanalysed [78] to take into account improved knowledge of radiative corrections [79], interference effects [80, 81] and the electron mass shift [82]. The reanalysis resolves long-standing tensions between the CUSB and the MD-1 collaboration results, improving the knowledge of the $\Upsilon(1S)$ mass significantly in the PDG averages. Prior to PDG'24, the $\Upsilon(2S)$ mass average included the data from the ARGUS and Crystal Ball collaborations [77]. Reference [78] has also studied these data, changing the central value by $0.15 \text{ MeV}/c^2$. Neither the value given in Ref. [78] nor the original value obtained in Ref. [77] are included in the PDG'24 averages. Consequently, the uncertainty on the $\Upsilon(2S)$ mass has worsened from 0.3 to $0.5 \text{ MeV}/c^2$. The values of the $\Upsilon(2S)$ and $\Upsilon(3S)$ mass presented here agree well with those from Ref. [78]. The value of $m_{\Upsilon(2S)}$ also agrees with the value [78] obtained from the reanalysis of ARGUS and Crystal Ball data, $m_{\Upsilon(2S)} = 10\,022.7 \pm 0.4 \text{ MeV}/c^2$. For the mass differences, there are tensions in the results presented here compared to those of the BaBar collaboration [72, 83] at the level of $2 - 4\sigma$.²

²The measurements in Ref. [72] are not listed in the PDG averages.

Table 9: Masses and mass differences for the χ_b states from PDG'24 [57]. For the $\chi_b(1P)$ and $\chi_b(2P)$ states, the second uncertainty comes from the uncertainty on the $\Upsilon(2S)$ and $\Upsilon(3S)$ mass, respectively. The last column shows the values recalculated from the photon energy in the $\Upsilon(2S) \rightarrow \chi_b(1P)\gamma$ decays using the mass of $\Upsilon(2S)$ meson from PDG'24 [57] and their difference. This calculation ignores any correlation between the photon energy measurements.

Parameter	PDG'24 [57]	Recalculated
$m_{\chi_{b1}(1P)}$ [MeV/ c^2]	$9\,892.78 \pm 0.26 \pm 0.31$	$9\,892.92 \pm 0.33 \pm 0.50$
$m_{\chi_{b2}(1P)}$ [MeV/ c^2]	$9\,912.21 \pm 0.26 \pm 0.31$	$9\,912.35 \pm 0.29 \pm 0.50$
$m_{\chi_{b1}(2P)}$ [MeV/ c^2]	$10\,255.46 \pm 0.22 \pm 0.50$	
$m_{\chi_{b2}(2P)}$ [MeV/ c^2]	$10\,268.65 \pm 0.22 \pm 0.50$	
$\delta m_{\chi_b(1P)}$ [MeV/ c^2]	19.10 ± 0.25	19.42 ± 0.44
$\delta m_{\chi_b(2P)}$ [MeV/ c^2]	13.10 ± 0.24	

The first observation of the $\chi_b \rightarrow \Upsilon(1S)\mu^+\mu^-$ decays provides measurements of the masses of the χ_b states,

$$\begin{aligned}
 m_{\chi_{b1}(1P)} &= 9\,892.50 \pm 0.26 \pm 0.10 \pm 0.10 \text{ MeV}/c^2, \\
 m_{\chi_{b2}(1P)} &= 9\,911.92 \pm 0.29 \pm 0.11 \pm 0.10 \text{ MeV}/c^2, \\
 m_{\chi_{b1}(2P)} &= 10\,253.97 \pm 0.75 \pm 0.22 \pm 0.09 \text{ MeV}/c^2, \\
 m_{\chi_{b2}(2P)} &= 10\,269.67 \pm 0.67 \pm 0.22 \pm 0.09 \text{ MeV}/c^2,
 \end{aligned}$$

where the first uncertainty is statistical, the second systematic and the third from the knowledge of the $\Upsilon(1S)$ mass [57]. The corresponding mass splittings are

$$\begin{aligned}
 m_{\chi_{b2}(1P)} - m_{\chi_{b1}(1P)} &= 19.4 \pm 0.4 \text{ MeV}/c^2, \\
 m_{\chi_{b2}(2P)} - m_{\chi_{b1}(2P)} &= 15.7 \pm 1.0 \text{ MeV}/c^2.
 \end{aligned}$$

The systematic uncertainties for the mass splittings are negligible with respect to the statistical uncertainties, and are omitted. These measurements can be compared to the corresponding world averages, given PDG'24 [57] and shown in Table 9. The previous measurements were largely made using the photon energy measured in feed down transitions, such as $\Upsilon(2S) \rightarrow \chi_b(1P)\gamma$. In the PDG'24 these values have not been updated to be consistent with the quoted value of the $\Upsilon(2S)$ mass, which has a changed central value and worse precision. The third column in Table 9 shows the precision of the $\chi_b(1P)$ masses worsening, as discussed above.

The values obtained by this analysis are the most precise measurements of the $\chi_b(1P)$ masses to date – regardless of the inconsistency in the uncertainties quoted in PDG'24. They agree well with the previous measurements, made using the photon energy in $\Upsilon(2S) \rightarrow \chi_b(1P)\gamma$ radiative transitions, which are dominated by results from the CLEO collaboration [9] and have very different systematic uncertainties. The measurements of the $\chi_b(2P)$ masses have slightly worse precision than the PDG'24 values. Again, the systematic uncertainties are very different to previous measurements using the photon energy in $\Upsilon(3S) \rightarrow \chi_b(2P)\gamma$ radiative transitions. All the mass measurements agree well with the PDG'24 values. The uncertainties on the χ_b mass splittings are not yet competitive with world averages values, which are dominated by high-precision

measurements from the BaBar collaboration [8]. The central value for $\delta m_{\chi_b(1P)}$ is in good agreement with the PDG'24 value, with a precision factor of 1.6 worse. The precision for $\delta m_{\chi_b(2P)}$ splitting is about four times worse than the PDG'24 value. The central value agrees with the PDG'24 at the level of 2.6 standard deviations. The mass differences between the χ_b and $\Upsilon(1S)$ states are listed in Appendix B.

In summary, precise spectroscopy of the hidden-beauty system is reported. Precision measurements of the masses of the $\Upsilon(2S)$ and $\Upsilon(3S)$ states have been made using their decays to $\Upsilon(1S)\pi^+\pi^-$ and $\Upsilon(2S)\pi^+\pi^-$ final states, respectively. These measurements are competitive and are in agreement with the world averages. They improve the knowledge of these parameters significantly and with different systematic uncertainties with respect to measurements at e^+e^- colliders. In addition, the $\Upsilon(1S)\mu^+\mu^-$ system at low mass has been studied for the first time, complementing the LHCb search for tetraquarks at higher mass reported in Ref. [84]. This has allowed the $\chi_b(1P)$ and $\chi_b(2P)$ decay modes to be observed with high significance, leading to competitive measurements of the masses of these states. The latter measurements are statistically limited and can be improved using the larger dataset that will be collected with the upgraded LHCb detector [85, 86]. With a larger dataset, the natural widths of these states could also be probed, and it will be possible to study $\chi_b(3P)$ decays to the $\Upsilon(1S)\mu^+\mu^-$ and $\Upsilon(2S)\mu^+\mu^-$ final states.

Acknowledgements

We express our gratitude to our colleagues in the CERN accelerator departments for the excellent performance of the LHC. We thank the technical and administrative staff at the LHCb institutes. We acknowledge support from CERN and from the national agencies: CAPES, CNPq, FAPERJ and FINEP (Brazil); MOST and NSFC (China); CNRS/IN2P3 (France); BMBF, DFG and MPG (Germany); INFN (Italy); NWO (Netherlands); MNiSW and NCN (Poland); MCID/IFA (Romania); MICIU and AEI (Spain); SNSF and SER (Switzerland); NASU (Ukraine); STFC (United Kingdom); DOE NP and NSF (USA). We acknowledge the computing resources that are provided by CERN, IN2P3 (France), KIT and DESY (Germany), INFN (Italy), SURF (Netherlands), PIC (Spain), GridPP (United Kingdom), CSCS (Switzerland), IFIN-HH (Romania), CBPF (Brazil), and Polish WLCG (Poland). We are indebted to the communities behind the multiple open-source software packages on which we depend. Individual groups or members have received support from ARC and ARDC (Australia); Key Research Program of Frontier Sciences of CAS, CAS PIFI, CAS CCEPP, Fundamental Research Funds for the Central Universities, and Sci. & Tech. Program of Guangzhou (China); Minciencias (Colombia); EPLANET, Marie Skłodowska-Curie Actions, ERC and NextGenerationEU (European Union); A*MIDEX, ANR, IPhU and Labex P2IO, and Région Auvergne-Rhône-Alpes (France); AvH Foundation (Germany); ICSC (Italy); Severo Ochoa and María de Maeztu Units of Excellence, GVA, XuntaGal, GENCAT, InTalent-Inditex and Prog. Atracción Talento CM (Spain); SRC (Sweden); the Leverhulme Trust, the Royal Society and UKRI (United Kingdom).

A Combination of results in the dimuon and dipion channels

The measurements of the mass splittings between the Υ states using the $\Upsilon \rightarrow \mu^+ \mu^-$ decays, Eqs. (5), and using the $\Upsilon(2S) \rightarrow \Upsilon(1S) \pi^+ \pi^-$ and $\Upsilon(3S) \rightarrow \Upsilon(2S) \pi^+ \pi^-$ decays, Eqs. (7) and (9), are in good agreement. They are combined assuming the uncertainty due to the momentum scale is fully correlated. This gives

$$m_{\Upsilon(2S)} - m_{\Upsilon(1S)} = 562.84 \pm 0.02 \pm 0.13 \text{ MeV}/c^2, \quad (\text{A1a})$$

$$m_{\Upsilon(3S)} - m_{\Upsilon(2S)} = 331.86 \pm 0.03 \pm 0.05 \text{ MeV}/c^2. \quad (\text{A1b})$$

The dipion modes dominate the determination of the averages.

B Mass differences for the χ_b and $\Upsilon(1S)$ states

The χ_b mass measurements, made using the known value of the mass of the $\Upsilon(1S)$ meson, are equivalent to the measurement of the mass differences:

$$m_{\chi_{b1}(1P)} - m_{\Upsilon(1S)} = 432.10 \pm 0.26 \pm 0.10 \text{ MeV}/c^2, \quad (\text{B2a})$$

$$m_{\chi_{b2}(1P)} - m_{\Upsilon(1S)} = 451.52 \pm 0.29 \pm 0.11 \text{ MeV}/c^2, \quad (\text{B2b})$$

$$m_{\chi_{b1}(2P)} - m_{\Upsilon(1S)} = 793.57 \pm 0.75 \pm 0.22 \text{ MeV}/c^2, \quad (\text{B2c})$$

$$m_{\chi_{b2}(2P)} - m_{\Upsilon(1S)} = 809.27 \pm 0.67 \pm 0.22 \text{ MeV}/c^2. \quad (\text{B2d})$$

While the systematic uncertainties on the χ_b masses in Table 6 are dominated by the momentum scale and hence highly correlated, the statistical correlations are small, less than 1% for the $m_{\chi_{b1}(1P)}$ and $m_{\chi_{b2}(1P)}$ states, and 6% for the $m_{\chi_{b1}(2P)}$ and $m_{\chi_{b2}(2P)}$ states.

References

- [1] E. Eichten *et al.*, *Charmonium: The model*, *Phys. Rev.* **D17** (1978) 3090, Erratum *ibid.* **D21** (1980) 313.
- [2] S. Godfrey and K. Moats, *Bottomonium mesons and strategies for their observation*, *Phys. Rev.* **D92** (2015) 054034, [arXiv:1507.00024](#).
- [3] J. Ferretti and E. Santopinto, *Higher mass bottomonia*, *Phys. Rev.* **D90** (2014) 094022, [arXiv:1306.2874](#).
- [4] J.-Z. Wang, Z.-F. Sun, X. Liu, and T. Matsuki, *Higher bottomonium zoo*, *Eur. Phys. J.* **C78** (2018) 915, [arXiv:1802.04938](#).
- [5] N. Brambilla *et al.*, *Heavy quarkonium: Progress, puzzles, and opportunities*, *Eur. Phys. J.* **C71** (2011) 1534, [arXiv:1010.5827](#).
- [6] F. Gross *et al.*, *50 Years of Quantum Chromodynamics*, *Eur. Phys. J.* **C83** (2023) 1125, [arXiv:2212.11107](#).
- [7] LHCb collaboration, R. Aaij *et al.*, χ_{c1} and χ_{c2} resonance parameters with the decays $\chi_{c1,c2} \rightarrow J/\psi \mu^+ \mu^-$, *Phys. Rev. Lett.* **119** (2017) 221801, [arXiv:1709.04247](#).
- [8] BaBar collaboration, J. P. Lees *et al.*, *Bottomonium spectroscopy and radiative transitions involving the $\chi_{bJ}(1P, 2P)$ states at BaBar*, *Phys. Rev.* **D90** (2014) 112010, [arXiv:1410.3902](#).
- [9] CLEO collaboration, M. Artuso *et al.*, *Photon transitions in $\Upsilon(2S)$ and $\Upsilon(3S)$ decays*, *Phys. Rev. Lett.* **94** (2005) 032001, [arXiv:hep-ex/0411068](#).
- [10] Crystal Ball collaboration, W. S. Walk *et al.*, *The χ_b states in exclusive radiative decay of the $\Upsilon(2S)$* , *Phys. Rev.* **D34** (1986) 2611.
- [11] ARGUS collaboration, H. Albrecht *et al.*, *Radiative decays of the $\Upsilon(2S)$ into the three χ_b states.*, *Phys. Lett.* **B160** (1985) 331.
- [12] CUSB collaboration, U. Heintz *et al.*, $b\bar{b}$ spectroscopy from the $\Upsilon(3S)$ state, *Phys. Rev.* **D46** (1992) 1928.
- [13] LHCb collaboration, R. Aaij *et al.*, *Measurement of the $\chi_b(3P)$ mass and of the relative rate of $\chi_{b1}(1P)$ and $\chi_{b2}(1P)$ production*, *JHEP* **10** (2014) 088, [arXiv:1409.1408](#).
- [14] LHCb collaboration, R. Aaij *et al.*, *Measurement of the W boson mass*, *JHEP* **01** (2022) 036, [arXiv:2109.01113](#).
- [15] LHCb collaboration, A. A. Alves Jr. *et al.*, *The LHCb detector at the LHC*, *JINST* **3** (2008) S08005.
- [16] LHCb collaboration, R. Aaij *et al.*, *LHCb detector performance*, *Int. J. Mod. Phys.* **A30** (2015) 1530022, [arXiv:1412.6352](#).
- [17] LHCb collaboration, R. Aaij *et al.*, *Momentum scale calibration of the LHCb spectrometer*, *JINST* **19** (2024) P02008, [arXiv:2312.01772](#).

- [18] LHCb collaboration, *LHCb muon system: Technical design report*, CERN-LHCC-2001-010, 2001.
- [19] A. A. Alves Jr. *et al.*, *Performance of the LHCb muon system*, JINST **8** (2013) P02022, [arXiv:1211.1346](#).
- [20] R. Aaij *et al.*, *The LHCb trigger and its performance in 2011*, JINST **8** (2013) P04022, [arXiv:1211.3055](#).
- [21] R. Aaij *et al.*, *Design and performance of the LHCb trigger and full real-time reconstruction in Run 2 of the LHC*, JINST **14** (2019) P04013, [arXiv:1812.10790](#).
- [22] S. Borghi, *Novel real-time alignment and calibration of the LHCb detector and its performance*, Nucl. Instrum. Meth. **A845** (2017) 560.
- [23] G. A. Cowan, D. C. Craik, and M. D. Needham, *RAPIDSIM: An application for the fast simulation of heavy-quark hadron decays*, Comput. Phys. Commun. **214** (2017) 239, [arXiv:1612.07489](#).
- [24] Geant4 collaboration, S. Agostinelli *et al.*, *GEANT4: A simulation toolkit*, Nucl. Instrum. Meth. **A506** (2003) 250.
- [25] Geant4 collaboration, J. Allison *et al.*, *GEANT4 developments and applications*, IEEE Trans. Nucl. Sci. **53** (2006) 270.
- [26] M. Clemencic *et al.*, *The LHCb simulation application, GAUSS: Design, evolution and experience*, J. Phys. Conf. Ser. **331** (2011) 032023.
- [27] D. J. Lange, *The EVTGEN particle decay simulation package*, Nucl. Instrum. Meth. **A462** (2001) 152.
- [28] P. Golonka and Z. Was, *PHOTOS Monte Carlo: A precision tool for QED corrections in Z and W decays*, Eur. Phys. J. **C45** (2006) 97, [arXiv:hep-ph/0506026](#).
- [29] N. Davidson, T. Przedzinski, and Z. Was, *PHOTOS interface in C++: Technical and physics documentation*, Comp. Phys. Comm. **199** (2016) 86, [arXiv:1011.0937](#).
- [30] L. S. Brown and R. N. Cahn, *Chiral symmetry and $\psi' \rightarrow \psi\pi\pi$ decay*, Phys. Rev. Lett. **35** (1975) 1.
- [31] M. B. Voloshin, *Two-pion transitions in quarkonium revisited*, Phys. Rev. **D74** (2006) 054022, [arXiv:hep-ph/0606258](#).
- [32] M. B. Voloshin, *Charmonium*, Prog. Part. Nucl. Phys. **61** (2008) 455, [arXiv:0711.4556](#).
- [33] A. V. Luchinsky, *Muon pair production in radiative decays of heavy quarkonia*, Mod. Phys. Lett. **A33** (2017) 1850001, [arXiv:1709.02444](#).
- [34] LHCb collaboration, R. Aaij *et al.*, *Measurement of Υ production in pp collisions at $\sqrt{s} = 7$ TeV*, Eur. Phys. J. **C72** (2012) 2025, [arXiv:1202.6579](#).


- [35] LHCb collaboration, R. Aaij *et al.*, *Production of J/ψ and Υ mesons in pp collisions at $\sqrt{s} = 8$ TeV*, *JHEP* **06** (2013) 064, [arXiv:1304.6977](#).
- [36] LHCb collaboration, R. Aaij *et al.*, *Measurement of Υ production in pp collisions at $\sqrt{s} = 2.76$ TeV*, *Eur. Phys. J.* **C74** (2014) 2835, [arXiv:1402.2539](#).
- [37] LHCb collaboration, R. Aaij *et al.*, *Forward production of Υ mesons in pp collisions at $\sqrt{s} = 7$ and 8 TeV*, *JHEP* **11** (2015) 103, [arXiv:1509.02372](#).
- [38] LHCb collaboration, R. Aaij *et al.*, *Measurement of Υ production cross-section in pp collisions at $\sqrt{s} = 13$ TeV*, *JHEP* **07** (2018) 134, [arXiv:1804.09214](#).
- [39] L. Breiman, J. H. Friedman, R. A. Olshen, and C. J. Stone, *Classification and regression trees*, Wadsworth international group, Belmont, California, USA, 1984.
- [40] Y. Freund and R. E. Schapire, *A decision-theoretic generalization of on-line learning and an application to boosting*, *J. Comput. Syst. Sci.* **55** (1997) 119.
- [41] H. Voss, A. Höcker, J. Stelzer, and F. Tegenfeldt, *TMVA – Toolkit for multivariate data analysis with ROOT*, *PoS ACAT* (2007) 040.
- [42] A. Höcker *et al.*, *TMVA 4 – Toolkit for multivariate data analysis with ROOT. Users guide.*, [arXiv:physics/0703039](#).
- [43] M. Pivk and F. R. Le Diberder, *sPlot: A statistical tool to unfold data distributions*, *Nucl. Instrum. Meth.* **A555** (2005) 356, [arXiv:physics/0402083](#).
- [44] LHCb collaboration, R. Aaij *et al.*, *Measurement of the track reconstruction efficiency at LHCb*, *JINST* **10** (2015) P02007, [arXiv:1408.1251](#).
- [45] R. Arink *et al.*, *Performance of the LHCb Outer Tracker*, *JINST* **9** (2014) P01002, [arXiv:1311.3893](#).
- [46] P. d'Argent *et al.*, *Improved performance of the LHCb Outer Tracker in LHC Run 2*, *JINST* **12** (2017) P11016, [arXiv:1708.00819](#).
- [47] M. De Cian, S. Farry, P. Seyfert, and S. Stahl, *Fast neural-net based fake track rejection in the LHCb reconstruction*, [LHCb-PUB-2017-011](#), 2017.
- [48] A. Powell *et al.*, *Particle identification at LHCb*, *PoS ICHEP2010* (2010) 020, [LHCb-PROC-2011-008](#).
- [49] T. Skwarnicki, *A study of the radiative cascade transitions between the Υ' and Υ resonances*, PhD thesis, Institute of Nuclear Physics, Krakow, 1986, [DESY-F31-86-02](#).
- [50] LHCb collaboration, R. Aaij *et al.*, *Observation of J/ψ -pair production in pp collisions at $\sqrt{s} = 7$ TeV*, *Phys. Lett.* **B707** (2012) 52, [arXiv:1109.0963](#).
- [51] LHCb collaboration, R. Aaij *et al.*, *Precision measurement of D meson mass differences*, *JHEP* **06** (2013) 065, [arXiv:1304.6865](#).

- [52] LHCb collaboration, R. Aaij *et al.*, *Measurement of b-hadron masses*, *Phys. Lett. B* **708** (2012) 241, [arXiv:1112.4896](#).
- [53] LHCb collaboration, R. Aaij *et al.*, *Study of Υ production and cold nuclear matter effects in pPb collisions at $\sqrt{s_{\text{NN}}} = 5$ TeV*, *JHEP* **07** (2014) 094, [arXiv:1405.5152](#).
- [54] LHCb collaboration, R. Aaij *et al.*, *Production of associated Υ and open charm hadrons in pp collisions at $\sqrt{s} = 7$ and 8 TeV via double parton scattering*, *JHEP* **07** (2016) 052, [arXiv:1510.05949](#).
- [55] LHCb collaboration, R. Aaij *et al.*, *Measurement of the $\Upsilon(nS)$ polarizations in pp collisions at $\sqrt{s} = 7$ and 8 TeV*, *JHEP* **12** (2017) 110, [arXiv:1709.01301](#).
- [56] M. Adinolfi *et al.*, *Performance of the LHCb RICH detector at the LHC*, *Eur. Phys. J. C* **73** (2013) 2431, [arXiv:1211.6759](#).
- [57] Particle Data Group, S. Navas *et al.*, *Review of particle physics*, *Phys. Rev. D* **110** (2024) 030001.
- [58] W. D. Hulsbergen, *Decay chain fitting with a Kalman filter*, *Nucl. Instrum. Meth. A* **552** (2005) 566, [arXiv:physics/0503191](#).
- [59] LHCb collaboration, R. Aaij *et al.*, *Study of the line shape of the $\chi_{c1}(3872)$ state*, *Phys. Rev. D* **102** (2020) 092005, [arXiv:2005.13419](#).
- [60] LHCb collaboration, R. Aaij *et al.*, *Study of the $\psi_2(3823)$ and $\chi_{c1}(3872)$ states in $B^+ \rightarrow (J/\psi\pi^+\pi^-)K^+$ decays*, *JHEP* **08** (2020) 123, [arXiv:2005.13422](#).
- [61] LHCb collaboration, R. Aaij *et al.*, *Study of $B_s^0 \rightarrow J/\psi\pi^+\pi^-K^+K^-$ decays*, *JHEP* **02** (2021) 024, [arXiv:2011.01867](#).
- [62] LHCb collaboration, R. Aaij *et al.*, *Observation of an exotic narrow doubly charmed tetraquark*, *Nature Physics* **18** (2022) 751, [arXiv:2109.01038](#).
- [63] LHCb collaboration, R. Aaij *et al.*, *Study of the doubly charmed tetraquark T_{cc}^+* , *Nature Communications* **13** (2022) 3351, [arXiv:2109.01056](#).
- [64] ARGUS collaboration, H. Albrecht *et al.*, *The hadronic transitions from $\Upsilon(2S)$ to $\Upsilon(1S)$* , *Z. Phys. C* **35** (1987) 283.
- [65] CLEO collaboration, F. Butler *et al.*, *Analysis of hadronic transitions in $\Upsilon(3S)$ decays*, *Phys. Rev. D* **49** (1994) 40.
- [66] J. Segovia, P. G. Ortega, D. R. Entem, and F. Fernández, *Bottomonium spectrum revisited*, *Phys. Rev. D* **93** (2016) 074027, [arXiv:1601.05093](#).
- [67] W.-J. Deng, H. Liu, L.-C. Gui, and X.-H. Zhong, *Spectrum and electromagnetic transitions of bottomonium*, *Phys. Rev. D* **95** (2017) 074002, [arXiv:1607.04696](#).
- [68] I. Asghar and N. Akbar, *Spectrum and decay properties of bottomonium mesons*, *Eur. Phys. J. A* **60** (2024) 58, [arXiv:2309.15438](#).

- [69] S. S. Wilks, *The large-sample distribution of the likelihood ratio for testing composite hypotheses*, [Ann. Math. Stat. **9** \(1938\) 60](#).
- [70] E. Byckling and K. Kajantie, *Particle kinematics*, John Wiley & Sons Inc., New York, 1973.
- [71] Particle Data Group, R. L. Workman *et al.*, *Review of particle physics*, [Prog. Theor. Exp. Phys. **2022** \(2022\) 083C01](#).
- [72] BaBar collaboration, J. P. Lees *et al.*, *Study of $\Upsilon(3S, 2S) \rightarrow \eta\Upsilon(1S)$ and $\Upsilon(3S, 2S) \rightarrow \pi^+\pi^-\Upsilon(1S)$ hadronic transitions*, [Phys. Rev. **D84** \(2011\) 092003](#), [arXiv:1108.5874](#).
- [73] MD-1 collaboration, A. S. Artamonov *et al.*, *A high precision measurement of the Υ , Υ' and Υ'' meson masses*, [Phys. Lett. **B137** \(1984\) 272](#).
- [74] MD-1 collaboration, S. E. Baru *et al.*, *New measurement of the Υ meson mass*, [Z. Phys. **C30** \(1986\) 551](#), Erratum [ibid. **C32** \(1986\) 622](#).
- [75] MD-1 collaboration, S. E. Baru *et al.*, *Determination of the $\Upsilon(1S)$ leptonic width*, [Z. Phys. **C56** \(1992\) 547](#).
- [76] W. W. MacKay *et al.* and CUSB collaboration, *Measurement of the Υ mass*, [Phys. Rev. **D29** \(1984\) 2483](#).
- [77] D. P. Barber *et al.* and ARGUS and Crystal Ball collaborations, *A precision measurement of the Υ' meson mass*, [Phys. Lett. **B135** \(1984\) 498](#).
- [78] A. G. Shamov and O. L. Rezanova, *Revision of results on $\Upsilon(1S)$, $\Upsilon(2S)$, and $\Upsilon(3S)$ masses*, [Phys. Lett. **B839** \(2023\) 137766](#), [arXiv:2210.13930](#).
- [79] E. A. Kuraev and V. S. Fadin, *On radiative corrections to e^+e^- single photon annihilation at high-energy*, [Sov. J. Nucl. Phys. **41** \(1985\) 466](#).
- [80] Y. I. Azimov, A. I. Vainshtein, L. N. Lipatov, and V. A. Khoze, *Electromagnetic corrections to the production of narrow resonances in colliding e^+e^- beams*, [Pisma Zh. Eksp. Teor. Fiz. **21** \(1975\) 378](#).
- [81] KEDR collaboration, V. V. Anashin *et al.*, *Measurement of main parameters of the $\psi(2S)$ resonance*, [Phys. Lett. **B711** \(2012\) 280](#), [arXiv:1109.4215](#).
- [82] E. R. Cohen and B. N. Taylor, *The 1986 adjustment of the fundamental physical constants*, [Rev. Mod. Phys. **59** \(1987\) 1121](#).
- [83] BaBar collaboration, J. P. Lees *et al.*, *Study of di-pion bottomonium transitions and search for the $h_b(1P)$ state*, [Phys. Rev. **D84** \(2011\) 011104](#), [arXiv:1105.4234](#).
- [84] LHCb collaboration, R. Aaij *et al.*, *Search for beautiful tetraquarks in the $\Upsilon(1S)\mu^+\mu^-$ invariant-mass spectrum*, [JHEP **10** \(2018\) 086](#), [arXiv:1806.09707](#).
- [85] LHCb collaboration, R. Aaij *et al.*, *The LHCb Upgrade I*, [JINST **19** \(2024\) P05065](#), [arXiv:2305.10515](#).
- [86] LHCb collaboration, *LHCb Framework TDR for the LHCb Upgrade II: Opportunities in flavour physics, and beyond, in the HL-LHC era*, [CERN-LHCC-2021-012](#), 2022.

LHCb collaboration

R. Aaij³⁷ , A.S.W. Abdelmotteleb⁵⁶ , C. Abellan Beteta⁵⁰ , F. Abudinén⁵⁶ ,
T. Ackernley⁶⁰ , A. A. Adefisoye⁶⁸ , B. Adeva⁴⁶ , M. Adinolfi⁵⁴ , P. Adlarson⁸¹ ,
C. Agapopoulou¹⁴ , C.A. Aidala⁸² , Z. Ajaltouni¹¹ , S. Akar⁶⁵ , K. Akiba³⁷ ,
P. Albicocco²⁷ , J. Albrecht¹⁹ , F. Alessio⁴⁸ , M. Alexander⁵⁹ , Z. Aliouche⁶² ,
P. Alvarez Cartelle⁵⁵ , R. Amalric¹⁶ , S. Amato³ , J.L. Amey⁵⁴ , Y. Amhis^{14,48} ,
L. An⁶ , L. Anderlini²⁶ , M. Andersson⁵⁰ , A. Andreianov⁴³ , P. Andreola⁵⁰ ,
M. Andreotti²⁵ , D. Andreou⁶⁸ , A. Anelli^{30,o} , D. Ao⁷ , F. Archilli^{36,u} ,
M. Argenton²⁵ , S. Arguedas Cuendis^{9,48} , A. Artamonov⁴³ , M. Artuso⁶⁸ ,
E. Aslanides¹³ , R. Ataíde Da Silva⁴⁹ , M. Atzeni⁶⁴ , B. Audurier¹⁵ , D. Bacher⁶³ ,
I. Bachiller Perea¹⁰ , S. Bachmann²¹ , M. Bachmayer⁴⁹ , J.J. Back⁵⁶ ,
P. Baladron Rodriguez⁴⁶ , V. Balagura¹⁵ , W. Baldini²⁵ , L. Balzani¹⁹ , H. Bao⁷ ,
J. Baptista de Souza Leite⁶⁰ , C. Barbero Pretel⁴⁶ , M. Barbetti²⁶ , I. R. Barbosa⁶⁹ ,
R.J. Barlow⁶² , M. Barnyakov²⁴ , S. Barsuk¹⁴ , W. Barter⁵⁸ , M. Bartolini⁵⁵ ,
J. Bartz⁶⁸ , J.M. Basels¹⁷ , S. Bashir³⁹ , G. Bassi^{34,r} , B. Batsukh⁵ , P. B. Battista¹⁴ ,
A. Bay⁴⁹ , A. Beck⁵⁶ , M. Becker¹⁹ , F. Bedeschi³⁴ , I.B. Bediaga² , N. B. Behling¹⁹ ,
S. Belin⁴⁶ , V. Bellec⁵⁰ , K. Belous⁴³ , I. Belov²⁸ , I. Belyaev³⁵ , G. Benane¹³ ,
G. Bencivenni²⁷ , E. Ben-Haim¹⁶ , A. Berezhnoy⁴³ , R. Bernet⁵⁰ , S. Bernet Andres⁴⁴ ,
A. Bertolin³² , C. Betancourt⁵⁰ , F. Betti⁵⁸ , J. Bex⁵⁵ , Ia. Bezshyiko⁵⁰ , J. Bhom⁴⁰ ,
M.S. Bieker¹⁹ , N.V. Biesuz²⁵ , P. Billoir¹⁶ , A. Biolchini³⁷ , M. Birch⁶¹ ,
F.C.R. Bishop¹⁰ , A. Bitadze⁶² , A. Bizzeti , T. Blake⁵⁶ , F. Blanc⁴⁹ , J.E. Blank¹⁹ ,
S. Blusk⁶⁸ , V. Bocharnikov⁴³ , J.A. Boelhaue¹⁹ , O. Boente Garcia¹⁵ ,
T. Boettcher⁶⁵ , A. Bohare⁵⁸ , A. Boldyrev⁴³ , C.S. Bolognani⁷⁸ , R. Bolzonella^{25,l} ,
N. Bondar⁴³ , A. Bordelius⁴⁸ , F. Borgato^{32,p} , S. Borghi⁶² , M. Borsato^{30,o} ,
J.T. Borsuk⁴⁰ , S.A. Bouchiba⁴⁹ , M. Bovill⁶³ , T.J.V. Bowcock⁶⁰ , A. Boyer⁴⁸ ,
C. Bozzi²⁵ , A. Brea Rodriguez⁴⁹ , N. Breer¹⁹ , J. Brodzicka⁴⁰ ,
A. Brossa Gonzalo^{46,56,45,†} , J. Brown⁶⁰ , D. Brundu³¹ , E. Buchanan⁵⁸ , A. Buonauro⁵⁰ ,
L. Buonincontri^{32,p} , A.T. Burke⁶² , C. Burr⁴⁸ , J.S. Butter⁵⁵ , J. Buytaert⁴⁸ ,
W. Byczynski⁴⁸ , S. Cadeddu³¹ , H. Cai⁷³ , A. C. Caillet¹⁶ , R. Calabrese^{25,l} ,
S. Calderon Ramirez⁹ , L. Calefice⁴⁵ , S. Cali²⁷ , M. Calvi^{30,o} , M. Calvo Gomez⁴⁴ ,
P. Camargo Magalhaes^{2,y} , J. I. Cambon Bouzas⁴⁶ , P. Campana²⁷ ,
D.H. Campora Perez⁷⁸ , A.F. Campoverde Quezada⁷ , S. Capelli³⁰ , L. Capriotti²⁵ ,
R. Caravaca-Mora⁹ , A. Carbone^{24,j} , L. Carcedo Salgado⁴⁶ , R. Cardinale^{28,m} ,
A. Cardini³¹ , P. Carniti^{30,o} , L. Carus²¹ , A. Casais Vidal⁶⁴ , R. Caspary²¹ ,
G. Casse⁶⁰ , J. Castro Godinez⁹ , M. Cattaneo⁴⁸ , G. Cavallero^{25,48} , V. Cavallini^{25,l} ,
S. Celani²¹ , D. Cervenkov⁶³ , S. Cesare^{29,n} , A.J. Chadwick⁶⁰ , I. Chahrouh⁸² ,
M. Charles¹⁶ , Ph. Charpentier⁴⁸ , E. Chatzianagnostou³⁷ , M. Chefdeville¹⁰ ,
C. Chen¹³ , S. Chen⁵ , Z. Chen⁷ , A. Chernov⁴⁰ , S. Chernyshenko⁵² , X.
Chiotopoulos⁷⁸ , V. Chobanova⁸⁰ , S. Cholak⁴⁹ , M. Chrzaszcz⁴⁰ , A. Chubykin⁴³ ,
V. Chulikov⁴³ , P. Ciambone²⁷ , X. Cid Vidal⁴⁶ , G. Ciezarek⁴⁸ , P. Cifra⁴⁸ ,
P.E.L. Clarke⁵⁸ , M. Clemencic⁴⁸ , H.V. Cliff⁵⁵ , J. Closier⁴⁸ , C. Cocha Toapaxi²¹ ,
V. Coco⁴⁸ , J. Cogan¹³ , E. Cogneras¹¹ , L. Cojocariu⁴² , P. Collins⁴⁸ ,
T. Colombo⁴⁸ , M. C. Colonna¹⁹ , A. Comerma-Montells⁴⁵ , L. Congedo²³ ,
A. Contu³¹ , N. Cooke⁵⁹ , I. Corredoira⁴⁶ , A. Correia¹⁶ , G. Corti⁴⁸ ,
J.J. Cottee Meldrum⁵⁴ , B. Couturier⁴⁸ , D.C. Craik⁵⁰ , M. Cruz Torres^{2,g} ,
E. Curras Rivera⁴⁹ , R. Currie⁵⁸ , C.L. Da Silva⁶⁷ , S. Dadabaev⁴³ , L. Dai⁷⁰ ,
X. Dai⁶ , E. Dall’Occo¹⁹ , J. Dalseno⁴⁶ , C. D’Ambrosio⁴⁸ , J. Daniel¹¹ ,
A. Danilina⁴³ , P. d’Argent²³ , A. Davidson⁵⁶ , J.E. Davies⁶² , A. Davis⁶² ,
O. De Aguiar Francisco⁶² , C. De Angelis^{31,k} , F. De Benedetti⁴⁸ , J. de Boer³⁷ ,

K. De Bruyn⁷⁷ , S. De Capua⁶² , M. De Cian^{21,48} , U. De Freitas Carneiro Da Graca^{2,b} ,
 E. De Lucia²⁷ , J.M. De Miranda² , L. De Paula³ , M. De Serio^{23,h} , P. De Simone²⁷ ,
 F. De Vellis¹⁹ , J.A. de Vries⁷⁸ , F. Debernardis²³ , D. Decamp¹⁰ , V. Dedu¹³ , S.
 Dekkers¹ , L. Del Buono¹⁶ , B. Delaney⁶⁴ , H.-P. Dembinski¹⁹ , J. Deng⁸ ,
 V. Denysenko⁵⁰ , O. Deschamps¹¹ , F. Dettori^{31,k} , B. Dey⁷⁶ , P. Di Nezza²⁷ ,
 I. Diachkov⁴³ , S. Didenko⁴³ , S. Ding⁶⁸ , L. Dittmann²¹ , V. Dobishuk⁵² , A. D.
 Docheva⁵⁹ , C. Dong^{4,c} , A.M. Donohoe²² , F. Dordei³¹ , A.C. dos Reis² , A. D.
 Dowling⁶⁸ , W. Duan⁷¹ , P. Duda⁷⁹ , M.W. Dudek⁴⁰ , L. Dufour⁴⁸ , V. Duk³³ ,
 P. Durante⁴⁸ , M. M. Duras⁷⁹ , J.M. Durham⁶⁷ , O. D. Durmus⁷⁶ , A. Dziurda⁴⁰ ,
 A. Dzyuba⁴³ , S. Easo⁵⁷ , E. Eckstein¹⁸ , U. Egede¹ , A. Egorychev⁴³ , V. Egorychev⁴³ ,
 S. Eisenhardt⁵⁸ , E. Ejopu⁶² , L. Eklund⁸¹ , M. Elashri⁶⁵ , J. Ellbracht¹⁹ , S. Ely⁶¹ ,
 A. Ene⁴² , E. Epple⁶⁵ , J. Eschle⁶⁸ , S. Esen²¹ , T. Evans⁶² , F. Fabiano^{31,k} ,
 L.N. Falcao² , Y. Fan⁷ , B. Fang⁷³ , L. Fantini^{33,q,48} , M. Faria⁴⁹ , K. Farmer⁵⁸ ,
 D. Fazzini^{30,o} , L. Felkowski⁷⁹ , M. Feng^{5,7} , M. Feo^{19,48} , A. Fernandez Casani⁴⁷ ,
 M. Fernandez Gomez⁴⁶ , A.D. Fernez⁶⁶ , F. Ferrari²⁴ , F. Ferreira Rodrigues³ ,
 M. Ferrillo⁵⁰ , M. Ferro-Luzzi⁴⁸ , S. Filippov⁴³ , R.A. Fini²³ , M. Fiorini^{25,l} ,
 M. Firlej³⁹ , K.L. Fischer⁶³ , D.S. Fitzgerald⁸² , C. Fitzpatrick⁶² , T. Fiutowski³⁹ ,
 F. Fleuret¹⁵ , M. Fontana²⁴ , L. F. Foreman⁶² , R. Forty⁴⁸ , D. Foulds-Holt⁵⁵ ,
 V. Franco Lima³ , M. Franco Sevilla⁶⁶ , M. Frank⁴⁸ , E. Franzoso^{25,l} , G. Frau⁶² ,
 C. Frei⁴⁸ , D.A. Friday⁶² , J. Fu⁷ , Q. Fuehring^{19,55} , Y. Fujii¹ , T. Fulghesu¹⁶ ,
 E. Gabriel³⁷ , G. Galati²³ , M.D. Galati³⁷ , A. Gallas Torreira⁴⁶ , D. Galli^{24,j} ,
 S. Gambetta⁵⁸ , M. Gandelman³ , P. Gandini²⁹ , B. Ganie⁶² , H. Gao⁷ , R. Gao⁶³ ,
 T.Q. Gao⁵⁵ , Y. Gao⁸ , Y. Gao⁶ , Y. Gao⁸ , M. Garau^{31,k} , L.M. Garcia Martin⁴⁹ ,
 P. Garcia Moreno⁴⁵ , J. García Pardiñas⁴⁸ , K. G. Garg⁸ , L. Garrido⁴⁵ , C. Gaspar⁴⁸ ,
 R.E. Geertsema³⁷ , L.L. Gerken¹⁹ , E. Gersabeck⁶² , M. Gersabeck⁶² , T. Gershon⁵⁶ ,
 S. G. Ghizzo²⁸ , Z. Ghorbanimoghaddam⁵⁴ , L. Giambastiani^{32,p} , F. I. Giasemis^{16,f} ,
 V. Gibson⁵⁵ , H.K. Giemza⁴¹ , A.L. Gilman⁶³ , M. Giovannetti²⁷ , A. Gioventù⁴⁵ ,
 L. Girardey⁶² , P. Gironella Gironell⁴⁵ , C. Giugliano^{25,l} , M.A. Giza⁴⁰ ,
 E.L. Gkoukousis⁶¹ , F.C. Glaser^{14,21} , V.V. Gligorov^{16,48} , C. Göbel⁶⁹ ,
 E. Golobardes⁴⁴ , D. Golubkov⁴³ , A. Golutvin^{61,43,48} , A. Gomes^{2,a,†} ,
 S. Gomez Fernandez⁴⁵ , F. Goncalves Abrantes⁶³ , M. Goncerz⁴⁰ , G. Gong^{4,c} , J.
 A. Gooding¹⁹ , I.V. Gorelov⁴³ , C. Gotti³⁰ , J.P. Grabowski¹⁸ ,
 L.A. Granado Cardoso⁴⁸ , E. Graugés⁴⁵ , E. Graverini^{49,s} , L. Grazette⁵⁶ ,
 G. Graziani , A. T. Grecu⁴² , L.M. Greeven³⁷ , N.A. Grieser⁶⁵ , L. Grillo⁵⁹ ,
 S. Gromov⁴³ , C. Gu¹⁵ , M. Guarise²⁵ , L. Guerry¹¹ , M. Guittiere¹⁴ ,
 V. Guliaeva⁴³ , P. A. Günther²¹ , A.-K. Guseinov⁴⁹ , E. Gushchin⁴³ , Y. Guz^{6,43,48} ,
 T. Gys⁴⁸ , K. Habermann¹⁸ , T. Hadavizadeh¹ , C. Hadjivasiliou⁶⁶ , G. Haefeli⁴⁹ ,
 C. Haen⁴⁸ , J. Haimberger⁴⁸ , M. Hajheidari⁴⁸ , G. H. Hallett⁵⁶ , M.M. Halvorsen⁴⁸ ,
 P.M. Hamilton⁶⁶ , J. Hammerich⁶⁰ , Q. Han⁸ , X. Han²¹ , S. Hansmann-Menzemer²¹ ,
 L. Hao⁷ , N. Harnew⁶³ , M. Hartmann¹⁴ , S. Hashmi³⁹ , J. He^{7,d} , F. Hemmer⁴⁸ ,
 C. Henderson⁶⁵ , R.D.L. Henderson^{1,56} , A.M. Hennequin⁴⁸ , K. Hennessy⁶⁰ ,
 L. Henry⁴⁹ , J. Herd⁶¹ , P. Herrero Gascon²¹ , J. Heuel¹⁷ , A. Hicheur³ ,
 G. Hijano Mendizabal⁵⁰ , D. Hill⁴⁹ , S.E. Hollitt¹⁹ , J. Horswill⁶² , R. Hou⁸ , Y. Hou¹¹ ,
 N. Howarth⁶⁰ , J. Hu²¹ , J. Hu⁷¹ , W. Hu⁶ , X. Hu^{4,c} , W. Huang⁷ , W. Hulsbergen³⁷ ,
 R.J. Hunter⁵⁶ , M. Hushchyn⁴³ , D. Hutchcroft⁶⁰ , M. Idzik³⁹ , D. Ilin⁴³ , P. Ilten⁶⁵ ,
 A. Inglese⁴³ , A. Iniukhin⁴³ , A. Ishteev⁴³ , K. Ivshin⁴³ , R. Jacobsson⁴⁸ , H. Jage¹⁷ ,
 S.J. Jaimes Elles^{47,74} , S. Jakobsen⁴⁸ , E. Jans³⁷ , B.K. Jashal⁴⁷ , A. Jawahery^{66,48} ,
 V. Jevtic¹⁹ , E. Jiang⁶⁶ , X. Jiang^{5,7} , Y. Jiang⁷ , Y. J. Jiang⁶ , M. John⁶³ , A.
 John Rubesh Rajan²² , D. Johnson⁵³ , C.R. Jones⁵⁵ , T.P. Jones⁵⁶ , S. Joshi⁴¹ ,
 B. Jost⁴⁸ , J. Juan Castella⁵⁵ , N. Jurik⁴⁸ , I. Juszcak⁴⁰ , D. Kaminaris⁴⁹ ,

S. Kandybei⁵¹ , M. Kane⁵⁸ , Y. Kang^{4,c} , C. Kar¹¹ , M. Karacson⁴⁸ ,
 D. Karpenkov⁴³ , A. Kauniskangas⁴⁹ , J.W. Kautz⁶⁵ , M.K. Kazanecki⁴⁰, F. Keizer⁴⁸ ,
 M. Kenzie⁵⁵ , T. Ketel³⁷ , B. Khanji⁶⁸ , A. Kharisova⁴³ , S. Kholodenko^{34,48} ,
 G. Khreich¹⁴ , T. Kirn¹⁷ , V.S. Kirsebom^{30,o} , O. Kitouni⁶⁴ , S. Klaver³⁸ ,
 N. Kleijne^{34,r} , K. Klimaszewski⁴¹ , M.R. Kmiec⁴¹ , S. Koliiev⁵² , L. Kolk¹⁹ ,
 A. Konoplyannikov⁴³ , P. Kopciwicz^{39,48} , P. Koppenburg³⁷ , M. Korolev⁴³ ,
 I. Kostyuk³⁷ , O. Kot⁵², S. Kotriakhova , A. Kozachuk⁴³ , P. Kravchenko⁴³ ,
 L. Kravchuk⁴³ , M. Kreps⁵⁶ , P. Krokovny⁴³ , W. Krupa⁶⁸ , W. Krzemien⁴¹ ,
 O.K. Kshyvanskyi⁵², S. Kubis⁷⁹ , M. Kucharczyk⁴⁰ , V. Kudryavtsev⁴³ , E. Kulikova⁴³ ,
 A. Kupsc⁸¹ , B. K. Kutsenko¹³ , D. Lacarrere⁴⁸ , P. Laguarda Gonzalez⁴⁵ , A. Lai³¹ ,
 A. Lampis³¹ , D. Lancierini⁵⁵ , C. Landesa Gomez⁴⁶ , J.J. Lane¹ , R. Lane⁵⁴ ,
 G. Lanfranchi²⁷ , C. Langenbruch²¹ , J. Langer¹⁹ , O. Lantwin⁴³ , T. Latham⁵⁶ ,
 F. Lazzari^{34,s} , C. Lazzeroni⁵³ , R. Le Gac¹³ , H. Lee⁶⁰ , R. Lefèvre¹¹ , A. Leflat⁴³ ,
 S. Legotin⁴³ , M. Lehuraux⁵⁶ , E. Lemos Cid⁴⁸ , O. Leroy¹³ , T. Lesiak⁴⁰ , E. Lesser⁴⁸,
 B. Leverington²¹ , A. Li^{4,c} , C. Li¹³ , H. Li⁷¹ , K. Li⁸ , L. Li⁶² , M. Li⁸, P. Li⁷ ,
 P.-R. Li⁷² , Q. Li^{5,7} , S. Li⁸ , T. Li^{5,e} , T. Li⁷¹ , Y. Li⁸, Y. Li⁵ , Z. Lian^{4,c} ,
 X. Liang⁶⁸ , S. Libralon⁴⁷ , C. Lin⁷ , T. Lin⁵⁷ , R. Lindner⁴⁸ , V. Lisovskyi⁴⁹ ,
 R. Litvinov^{31,48} , F. L. Liu¹ , G. Liu⁷¹ , K. Liu⁷² , S. Liu^{5,7} , W. Liu⁸, Y. Liu⁵⁸ ,
 Y. Liu⁷², Y. L. Liu⁶¹ , A. Lobo Salvia⁴⁵ , A. Loi³¹ , J. Lomba Castro⁴⁶ , T. Long⁵⁵ ,
 J.H. Lopes³ , A. Lopez Huertas⁴⁵ , S. López Soliño⁴⁶ , Q. Lu¹⁵ , C. Lucarelli²⁶ ,
 D. Lucchesi^{32,p} , M. Lucio Martinez⁷⁸ , V. Lukashenko^{37,52} , Y. Luo⁶ , A. Lupato^{32,i} ,
 E. Luppi^{25,l} , K. Lynch²² , X.-R. Lyu⁷ , G. M. Ma^{4,c} , R. Ma⁷ , S. Maccolini¹⁹ ,
 F. Machefert¹⁴ , F. Maciuc⁴² , B. Mack⁶⁸ , I. Mackay⁶³ , L. M. Mackey⁶⁸ ,
 L.R. Madhan Mohan⁵⁵ , M. J. Madurai⁵³ , A. Maevskiy⁴³ , D. Magdalinski³⁷ ,
 D. Maisuzenko⁴³ , M.W. Majewski³⁹, J.J. Malczewski⁴⁰ , S. Malde⁶³ , L. Malentacca⁴⁸,
 A. Malinin⁴³ , T. Maltsev⁴³ , G. Manca^{31,k} , G. Mancinelli¹³ , C. Mancuso^{29,14,n} ,
 R. Manera Escalero⁴⁵, D. Manuzzi²⁴ , D. Marangotto^{29,n} , J.F. Marchand¹⁰ ,
 R. Marchevski⁴⁹ , U. Marconi²⁴ , E. Mariani¹⁶, S. Mariani⁴⁸ , C. Marin Benito⁴⁵ ,
 J. Marks²¹ , A.M. Marshall⁵⁴ , L. Martel⁶³ , G. Martelli^{33,q} , G. Martellotti³⁵ ,
 L. Martinazzoli⁴⁸ , M. Martinelli^{30,o} , D. Martinez Santos⁴⁶ , F. Martinez Vidal⁴⁷ ,
 A. Massafferri² , R. Matev⁴⁸ , A. Mathad⁴⁸ , V. Matiunin⁴³ , C. Matteuzzi⁶⁸ ,
 K.R. Mattioli¹⁵ , A. Mauri⁶¹ , E. Maurice¹⁵ , J. Mauricio⁴⁵ , P. Mayencourt⁴⁹ ,
 J. Mazorra de Cos⁴⁷ , M. Mazurek⁴¹ , M. McCann⁶¹ , L. McConnell²² ,
 T.H. McGrath⁶² , N.T. McHugh⁵⁹ , A. McNab⁶² , R. McNulty²² , B. Meadows⁶⁵ ,
 G. Meier¹⁹ , D. Melnychuk⁴¹ , F. M. Meng^{4,c} , M. Merk^{37,78} , A. Merli⁴⁹ ,
 L. Meyer Garcia⁶⁶ , D. Miao^{5,7} , H. Miao⁷ , M. Mikhasenko⁷⁵ , D.A. Milanes⁷⁴ ,
 A. Minotti^{30,o} , E. Minucci⁶⁸ , T. Miralles¹¹ , B. Mitreska¹⁹ , D.S. Mitzel¹⁹ ,
 A. Modak⁵⁷ , R.A. Mohammed⁶³ , R.D. Moise¹⁷ , S. Mokhnenko⁴³ , E.
 F. Molina Cardenas⁸² , T. Mombächer⁴⁸ , M. Monk^{56,1} , S. Monteil¹¹ ,
 A. Morcillo Gomez⁴⁶ , G. Morello²⁷ , M.J. Morello^{34,r} , M.P. Morgenthaler²¹ ,
 J. Moron³⁹ , A.B. Morris⁴⁸ , A.G. Morris¹³ , R. Mountain⁶⁸ , H. Mu^{4,c} , Z. M. Mu⁶ ,
 E. Muhammad⁵⁶ , F. Muheim⁵⁸ , M. Mulder⁷⁷ , K. Müller⁵⁰ , F. Muñoz-Rojas⁹ ,
 R. Murta⁶¹ , P. Naik⁶⁰ , T. Nakada⁴⁹ , R. Nandakumar⁵⁷ , T. Namut⁴⁸ , I. Nasteva³ ,
 M. Needham⁵⁸ , N. Neri^{29,n} , S. Neubert¹⁸ , N. Neufeld⁴⁸ , P. Neustroev⁴³,
 J. Nicolini^{19,14} , D. Nicotra⁷⁸ , E.M. Niel⁴⁹ , N. Nikitin⁴³ , P. Nogarolli³ , P. Nogga¹⁸,
 C. Normand⁵⁴ , J. Novoa Fernandez⁴⁶ , G. Nowak⁶⁵ , C. Nunez⁸² , H. N. Nur⁵⁹ ,
 A. Oblakowska-Mucha³⁹ , V. Obraztsov⁴³ , T. Oeser¹⁷ , S. Okamura^{25,l} ,
 A. Okhotnikov⁴³, O. Okhrimenko⁵² , R. Oldeman^{31,k} , F. Oliva⁵⁸ , M. Olocco¹⁹ ,
 C.J.G. Onderwater⁷⁸ , R.H. O'Neil⁵⁸ , D. Osthues¹⁹, J.M. Otalora Goicochea³ ,
 P. Owen⁵⁰ , A. Oyanguren⁴⁷ , O. Ozcelik⁵⁸ , F. Paciolla^{34,v} , A. Padee⁴¹ ,

K.O. Padeken¹⁸ , B. Pagare⁵⁶ , P.R. Pais²¹ , T. Pajero⁴⁸ , A. Palano²³ ,
 M. Palutan²⁷ , G. Panshin⁴³ , L. Paolucci⁵⁶ , A. Papanestis^{57,48} , M. Pappagallo^{23,h} ,
 L.L. Pappalardo^{25,l} , C. Pappenheimer⁶⁵ , C. Parkes⁶² , B. Passalacqua²⁵ ,
 G. Passaleva²⁶ , D. Passaro^{34,r} , A. Pastore²³ , M. Patel⁶¹ , J. Patoc⁶³ ,
 C. Patrignani^{24,j} , A. Paul⁶⁸ , C.J. Pawley⁷⁸ , A. Pellegrino³⁷ , J. Peng^{5,7} ,
 M. Pepe Altarelli²⁷ , S. Perazzini²⁴ , D. Pereima⁴³ , H. Pereira Da Costa⁶⁷ ,
 A. Pereiro Castro⁴⁶ , P. Perret¹¹ , A. Perro⁴⁸ , K. Petridis⁵⁴ , A. Petrolini^{28,m} , J. P.
 Pfaller⁶⁵ , H. Pham⁶⁸ , L. Pica^{34,r} , M. Piccini³³ , L. Piccolo³¹ , B. Pietrzyk¹⁰ ,
 G. Pietrzyk¹⁴ , D. Pinci³⁵ , F. Pisani⁴⁸ , M. Pizzichemi^{30,o} , V. Placinta⁴² ,
 M. Plo Casasus⁴⁶ , T. Poeschl⁴⁸ , F. Polci^{16,48} , M. Poli Lener²⁷ , A. Poluektov¹³ ,
 N. Polukhina⁴³ , I. Polyakov⁴³ , E. Polcarpo³ , S. Ponce⁴⁸ , D. Popov⁷ ,
 S. Poslavskii⁴³ , K. Prasanth⁵⁸ , C. Prouve⁴⁶ , D. Provenzano^{31,k} , V. Pugatch⁵² ,
 G. Punzi^{34,s} , S. Qasim⁵⁰ , Q. Q. Qian⁶ , W. Qian⁷ , N. Qin^{4,c} , S. Qu^{4,c} ,
 R. Quagliani⁴⁸ , R.I. Rabadan Trejo⁵⁶ , J.H. Rademacker⁵⁴ , M. Rama³⁴ , M.
 Ramírez García⁸² , V. Ramos De Oliveira⁶⁹ , M. Ramos Pernas⁵⁶ , M.S. Rangel³ ,
 F. Ratnikov⁴³ , G. Raven³⁸ , M. Rebollo De Miguel⁴⁷ , F. Redi^{29,i} , J. Reich⁵⁴ ,
 F. Reiss⁶² , Z. Ren⁷ , P.K. Resmi⁶³ , R. Ribatti⁴⁹ , G. R. Ricart^{15,12} ,
 D. Riccardi^{34,r} , S. Ricciardi⁵⁷ , K. Richardson⁶⁴ , M. Richardson-Slipper⁵⁸ ,
 K. Rinnert⁶⁰ , P. Robbe¹⁴ , G. Robertson⁵⁹ , E. Rodrigues⁶⁰ ,
 E. Rodriguez Fernandez⁴⁶ , J.A. Rodriguez Lopez⁷⁴ , E. Rodriguez Rodriguez⁴⁶ ,
 J. Roensch¹⁹ , A. Rogachev⁴³ , A. Rogovskiy⁵⁷ , D.L. Rolf⁴⁸ , P. Roloff⁴⁸ ,
 V. Romanovskiy⁶⁵ , M. Romero Lamas⁴⁶ , A. Romero Vidal⁴⁶ , G. Romolini²⁵ ,
 F. Ronchetti⁴⁹ , T. Rong⁶ , M. Rotondo²⁷ , S. R. Roy²¹ , M.S. Rudolph⁶⁸ ,
 M. Ruiz Diaz²¹ , R.A. Ruiz Fernandez⁴⁶ , J. Ruiz Vidal^{81,z} , A. Ryzhikov⁴³ ,
 J. Ryzka³⁹ , J. J. Saavedra-Arias⁹ , J.J. Saborido Silva⁴⁶ , R. Sadek¹⁵ , N. Sagidova⁴³ ,
 D. Sahoo⁷⁶ , N. Sahoo⁵³ , B. Saitta^{31,k} , M. Salomoni^{30,o,48} , I. Sanderswood⁴⁷ ,
 R. Santacesaria³⁵ , C. Santamarina Rios⁴⁶ , M. Santimaria^{27,48} , L. Santoro² ,
 E. Santovetti³⁶ , A. Saputi^{25,48} , D. Saranin⁴³ , A. Sarnatskiy⁷⁷ , G. Sarpis⁵⁸ ,
 M. Sarpis⁶² , C. Satriano^{35,t} , A. Satta³⁶ , M. Saur⁶ , D. Savrina⁴³ , H. Sazak¹⁷ ,
 L.G. Scantlebury Smead⁶³ , A. Scarabotto¹⁹ , S. Schael¹⁷ , S. Scherl⁶⁰ , M. Schiller⁵⁹ ,
 H. Schindler⁴⁸ , M. Schmelling²⁰ , B. Schmidt⁴⁸ , S. Schmitt¹⁷ , H. Schmitz¹⁸,
 O. Schneider⁴⁹ , A. Schopper⁴⁸ , N. Schulte¹⁹ , S. Schulte⁴⁹ , M.H. Schune¹⁴ ,
 R. Schwemmer⁴⁸ , G. Schwering¹⁷ , B. Sciascia²⁷ , A. Sciucati⁴⁸ , S. Sellam⁴⁶ ,
 A. Semennikov⁴³ , T. Senger⁵⁰ , M. Senghi Soares³⁸ , A. Sergi^{28,48} , N. Serra⁵⁰ ,
 L. Sestini³² , A. Seuthe¹⁹ , Y. Shang⁶ , D.M. Shangase⁸² , M. Shapkin⁴³ , R. S.
 Sharma⁶⁸ , I. Shchemerov⁴³ , L. Shchutska⁴⁹ , T. Shears⁶⁰ , L. Shekhtman⁴³ ,
 Z. Shen⁶ , S. Sheng^{5,7} , V. Shevchenko⁴³ , B. Shi⁷ , Q. Shi⁷ , Y. Shimizu¹⁴ ,
 E. Shmanin²⁴ , R. Shorkin⁴³ , J.D. Shupperd⁶⁸ , R. Silva Coutinho⁶⁸ , G. Simi^{32,p} ,
 S. Simone^{23,h} , N. Skidmore⁵⁶ , T. Skwarnicki⁶⁸ , M.W. Slater⁵³ , J.C. Smallwood⁶³ ,
 E. Smith⁶⁴ , K. Smith⁶⁷ , M. Smith⁶¹ , A. Snoch³⁷ , L. Soares Lavra⁵⁸ ,
 M.D. Sokoloff⁶⁵ , F.J.P. Soler⁵⁹ , A. Solomin^{43,54} , A. Solovev⁴³ , I. Solovyev⁴³ ,
 R. Song¹ , Y. Song⁴⁹ , Y. Song^{4,c} , Y. S. Song⁶ , F.L. Souza De Almeida⁶⁸ ,
 B. Souza De Paula³ , E. Spadaro Norella²⁸ , E. Spedicato²⁴ , J.G. Speer¹⁹ ,
 E. Spiridenkov⁴³ , P. Spradlin⁵⁹ , V. Srisakaran⁴⁸ , F. Stagni⁴⁸ , M. Stahl⁴⁸ , S. Stahl⁴⁸ ,
 S. Stanislaus⁶³ , E.N. Stein⁴⁸ , O. Steinkamp⁵⁰ , O. Stenyakin⁴³ , H. Stevens¹⁹ ,
 D. Strelakina⁴³ , Y. Su⁷ , F. Suljik⁶³ , J. Sun³¹ , L. Sun⁷³ , Y. Sun⁶⁶ ,
 D. Sundfeld² , W. Sutcliffe⁵⁰ , P.N. Swallow⁵³ , K. Swientek³⁹ , F. Swystun⁵⁵ ,
 A. Szabelski⁴¹ , T. Szumlak³⁹ , Y. Tan^{4,c} , M.D. Tat⁶³ , A. Terentev⁴³ ,
 F. Terzuoli^{34,v,48} , F. Teubert⁴⁸ , E. Thomas⁴⁸ , D.J.D. Thompson⁵³ , H. Tilquin⁶¹ ,
 V. Tisserand¹¹ , S. T'Jampens¹⁰ , M. Tobin^{5,48} , L. Tomassetti^{25,l} , G. Tonani^{29,n,48} ,

X. Tong⁶ , D. Torres Machado² , L. Toscano¹⁹ , D.Y. Tou^{4,c} , C. Trippel⁴⁴ , G. Tuci²¹ , N. Tuning³⁷ , L.H. Uecker²¹ , A. Ukleja³⁹ , D.J. Unverzagt²¹ , E. Ursov⁴³ , A. Usachov³⁸ , A. Ustyuzhanin⁴³ , U. Uwer²¹ , V. Vagnoni²⁴ , V. Valcarce Cadenas⁴⁶ , G. Valenti²⁴ , N. Valls Canudas⁴⁸ , H. Van Hecke⁶⁷ , E. van Herwijnen⁶¹ , C.B. Van Hulse^{46,x} , R. Van Laak⁴⁹ , M. van Veghel³⁷ , G. Vasquez⁵⁰ , R. Vazquez Gomez⁴⁵ , P. Vazquez Regueiro⁴⁶ , C. Vázquez Sierra⁴⁶ , S. Vecchi²⁵ , J.J. Velthuis⁵⁴ , M. Veltri^{26,w} , A. Venkateswaran⁴⁹ , M. Verdoglia³¹ , M. Vesterinen⁵⁶ , D. Vico Benet⁶³ , P. V. Vidrier Villalba⁴⁵ , M. Vieites Diaz⁴⁸ , X. Vilasis-Cardona⁴⁴ , E. Vilella Figueras⁶⁰ , A. Villa²⁴ , P. Vincent¹⁶ , F.C. Volle⁵³ , D. vom Bruch¹³ , N. Voropaev⁴³ , K. Vos⁷⁸ , G. Vouters¹⁰ , C. Vrahas⁵⁸ , J. Wagner¹⁹ , J. Walsh³⁴ , E.J. Walton^{1,56} , G. Wan⁶ , C. Wang²¹ , G. Wang⁸ , J. Wang⁶ , J. Wang⁵ , J. Wang^{4,c} , J. Wang⁷³ , M. Wang²⁹ , N. W. Wang⁷ , R. Wang⁵⁴ , X. Wang⁸ , X. Wang⁷¹ , X. W. Wang⁶¹ , Y. Wang⁶ , Z. Wang¹⁴ , Z. Wang^{4,c} , Z. Wang²⁹ , J.A. Ward^{56,1} , M. Waterlaet⁴⁸ , N.K. Watson⁵³ , D. Websdale⁶¹ , Y. Wei⁶ , J. Wendel⁸⁰ , B.D.C. Westhenry⁵⁴ , C. White⁵⁵ , M. Whitehead⁵⁹ , E. Whiter⁵³ , A.R. Wiederhold⁶² , D. Wiedner¹⁹ , G. Wilkinson⁶³ , M.K. Wilkinson⁶⁵ , M. Williams⁶⁴ , M.R.J. Williams⁵⁸ , R. Williams⁵⁵ , Z. Williams⁵⁴ , F.F. Wilson⁵⁷ , W. Wislicki⁴¹ , M. Witek⁴⁰ , L. Witola²¹ , G. Wormser¹⁴ , S.A. Wotton⁵⁵ , H. Wu⁶⁸ , J. Wu⁸ , Y. Wu⁶ , Z. Wu⁷ , K. Wyllie⁴⁸ , S. Xian⁷¹ , Z. Xiang⁵ , Y. Xie⁸ , A. Xu³⁴ , J. Xu⁷ , L. Xu^{4,c} , L. Xu^{4,c} , M. Xu⁵⁶ , Z. Xu⁴⁸ , Z. Xu⁷ , Z. Xu⁵ , D. Yang⁴ , K. Yang⁶¹ , S. Yang⁷ , X. Yang⁶ , Y. Yang^{28,m} , Z. Yang⁶ , Z. Yang⁶⁶ , V. Yeroshenko¹⁴ , H. Yeung⁶² , H. Yin⁸ , C. Y. Yu⁶ , J. Yu⁷⁰ , X. Yuan⁵ , Y. Yuan^{5,7} , E. Zaffaroni⁴⁹ , M. Zavertyaev²⁰ , M. Zdybal⁴⁰ , F. Zenesini^{24,j} , C. Zeng^{5,7} , M. Zeng^{4,c} , C. Zhang⁶ , D. Zhang⁸ , J. Zhang⁷ , L. Zhang^{4,c} , S. Zhang⁷⁰ , S. Zhang⁶³ , Y. Zhang⁶ , Y. Z. Zhang^{4,c} , Y. Zhao²¹ , A. Zharkova⁴³ , A. Zhelezov²¹ , S. Z. Zheng⁶ , X. Z. Zheng^{4,c} , Y. Zheng⁷ , T. Zhou⁶ , X. Zhou⁸ , Y. Zhou⁷ , V. Zhovkovska⁵⁶ , L. Z. Zhu⁷ , X. Zhu^{4,c} , X. Zhu⁸ , V. Zhukov¹⁷ , J. Zhuo⁴⁷ , Q. Zou^{5,7} , D. Zuliani^{32,p} , G. Zunica⁴⁹ .

¹*School of Physics and Astronomy, Monash University, Melbourne, Australia*

²*Centro Brasileiro de Pesquisas Físicas (CBPF), Rio de Janeiro, Brazil*

³*Universidade Federal do Rio de Janeiro (UFRJ), Rio de Janeiro, Brazil*

⁴*Department of Engineering Physics, Tsinghua University, Beijing, China, Beijing, China*

⁵*Institute Of High Energy Physics (IHEP), Beijing, China*

⁶*School of Physics State Key Laboratory of Nuclear Physics and Technology, Peking University, Beijing, China*

⁷*University of Chinese Academy of Sciences, Beijing, China*

⁸*Institute of Particle Physics, Central China Normal University, Wuhan, Hubei, China*

⁹*Consejo Nacional de Rectores (CONARE), San Jose, Costa Rica*

¹⁰*Université Savoie Mont Blanc, CNRS, IN2P3-LAPP, Annecy, France*

¹¹*Université Clermont Auvergne, CNRS/IN2P3, LPC, Clermont-Ferrand, France*

¹²*Département de Physique Nucléaire (SPhN), Gif-Sur-Yvette, France*

¹³*Aix Marseille Univ, CNRS/IN2P3, CPPM, Marseille, France*

¹⁴*Université Paris-Saclay, CNRS/IN2P3, IJCLab, Orsay, France*

¹⁵*Laboratoire Leprince-Ringuet, CNRS/IN2P3, Ecole Polytechnique, Institut Polytechnique de Paris, Palaiseau, France*

¹⁶*LPNHE, Sorbonne Université, Paris Diderot Sorbonne Paris Cité, CNRS/IN2P3, Paris, France*

¹⁷*I. Physikalisches Institut, RWTH Aachen University, Aachen, Germany*

¹⁸*Universität Bonn - Helmholtz-Institut für Strahlen und Kernphysik, Bonn, Germany*

¹⁹*Fakultät Physik, Technische Universität Dortmund, Dortmund, Germany*

²⁰*Max-Planck-Institut für Kernphysik (MPIK), Heidelberg, Germany*

²¹*Physikalisches Institut, Ruprecht-Karls-Universität Heidelberg, Heidelberg, Germany*

²²*School of Physics, University College Dublin, Dublin, Ireland*

- ²³ INFN Sezione di Bari, Bari, Italy
- ²⁴ INFN Sezione di Bologna, Bologna, Italy
- ²⁵ INFN Sezione di Ferrara, Ferrara, Italy
- ²⁶ INFN Sezione di Firenze, Firenze, Italy
- ²⁷ INFN Laboratori Nazionali di Frascati, Frascati, Italy
- ²⁸ INFN Sezione di Genova, Genova, Italy
- ²⁹ INFN Sezione di Milano, Milano, Italy
- ³⁰ INFN Sezione di Milano-Bicocca, Milano, Italy
- ³¹ INFN Sezione di Cagliari, Monserrato, Italy
- ³² INFN Sezione di Padova, Padova, Italy
- ³³ INFN Sezione di Perugia, Perugia, Italy
- ³⁴ INFN Sezione di Pisa, Pisa, Italy
- ³⁵ INFN Sezione di Roma La Sapienza, Roma, Italy
- ³⁶ INFN Sezione di Roma Tor Vergata, Roma, Italy
- ³⁷ Nikhef National Institute for Subatomic Physics, Amsterdam, Netherlands
- ³⁸ Nikhef National Institute for Subatomic Physics and VU University Amsterdam, Amsterdam, Netherlands
- ³⁹ AGH - University of Krakow, Faculty of Physics and Applied Computer Science, Kraków, Poland
- ⁴⁰ Henryk Niewodniczanski Institute of Nuclear Physics Polish Academy of Sciences, Kraków, Poland
- ⁴¹ National Center for Nuclear Research (NCBJ), Warsaw, Poland
- ⁴² Horia Hulubei National Institute of Physics and Nuclear Engineering, Bucharest-Magurele, Romania
- ⁴³ Affiliated with an institute covered by a cooperation agreement with CERN
- ⁴⁴ DS4DS, La Salle, Universitat Ramon Llull, Barcelona, Spain
- ⁴⁵ ICCUB, Universitat de Barcelona, Barcelona, Spain
- ⁴⁶ Instituto Galego de Física de Altas Enerxías (IGFAE), Universidade de Santiago de Compostela, Santiago de Compostela, Spain
- ⁴⁷ Instituto de Física Corpuscular, Centro Mixto Universidad de Valencia - CSIC, Valencia, Spain
- ⁴⁸ European Organization for Nuclear Research (CERN), Geneva, Switzerland
- ⁴⁹ Institute of Physics, Ecole Polytechnique Fédérale de Lausanne (EPFL), Lausanne, Switzerland
- ⁵⁰ Physik-Institut, Universität Zürich, Zürich, Switzerland
- ⁵¹ NSC Kharkiv Institute of Physics and Technology (NSC KIPT), Kharkiv, Ukraine
- ⁵² Institute for Nuclear Research of the National Academy of Sciences (KINR), Kyiv, Ukraine
- ⁵³ School of Physics and Astronomy, University of Birmingham, Birmingham, United Kingdom
- ⁵⁴ H.H. Wills Physics Laboratory, University of Bristol, Bristol, United Kingdom
- ⁵⁵ Cavendish Laboratory, University of Cambridge, Cambridge, United Kingdom
- ⁵⁶ Department of Physics, University of Warwick, Coventry, United Kingdom
- ⁵⁷ STFC Rutherford Appleton Laboratory, Didcot, United Kingdom
- ⁵⁸ School of Physics and Astronomy, University of Edinburgh, Edinburgh, United Kingdom
- ⁵⁹ School of Physics and Astronomy, University of Glasgow, Glasgow, United Kingdom
- ⁶⁰ Oliver Lodge Laboratory, University of Liverpool, Liverpool, United Kingdom
- ⁶¹ Imperial College London, London, United Kingdom
- ⁶² Department of Physics and Astronomy, University of Manchester, Manchester, United Kingdom
- ⁶³ Department of Physics, University of Oxford, Oxford, United Kingdom
- ⁶⁴ Massachusetts Institute of Technology, Cambridge, MA, United States
- ⁶⁵ University of Cincinnati, Cincinnati, OH, United States
- ⁶⁶ University of Maryland, College Park, MD, United States
- ⁶⁷ Los Alamos National Laboratory (LANL), Los Alamos, NM, United States
- ⁶⁸ Syracuse University, Syracuse, NY, United States
- ⁶⁹ Pontifícia Universidade Católica do Rio de Janeiro (PUC-Rio), Rio de Janeiro, Brazil, associated to ³
- ⁷⁰ School of Physics and Electronics, Hunan University, Changsha City, China, associated to ⁸
- ⁷¹ Guangdong Provincial Key Laboratory of Nuclear Science, Guangdong-Hong Kong Joint Laboratory of Quantum Matter, Institute of Quantum Matter, South China Normal University, Guangzhou, China, associated to
- ⁷² Lanzhou University, Lanzhou, China, associated to ⁵
- ⁷³ School of Physics and Technology, Wuhan University, Wuhan, China, associated to
- ⁷⁴ Departamento de Física, Universidad Nacional de Colombia, Bogota, Colombia, associated to ¹⁶

- ⁷⁵ *Ruhr Universitaet Bochum, Fakultaet f. Physik und Astronomie, Bochum, Germany, associated to* ¹⁹
⁷⁶ *Eotvos Lorand University, Budapest, Hungary, associated to* ⁴⁸
⁷⁷ *Van Swinderen Institute, University of Groningen, Groningen, Netherlands, associated to* ³⁷
⁷⁸ *Universiteit Maastricht, Maastricht, Netherlands, associated to* ³⁷
⁷⁹ *Tadeusz Kosciuszko Cracow University of Technology, Cracow, Poland, associated to* ⁴⁰
⁸⁰ *Universidade da Coruña, A Coruna, Spain, associated to* ⁴⁴
⁸¹ *Department of Physics and Astronomy, Uppsala University, Uppsala, Sweden, associated to* ⁵⁹
⁸² *University of Michigan, Ann Arbor, MI, United States, associated to* ⁶⁸

^a *Universidade de Brasília, Brasília, Brazil*

^b *Centro Federal de Educação Tecnológica Celso Suckow da Fonseca, Rio De Janeiro, Brazil*

^c *Center for High Energy Physics, Tsinghua University, Beijing, China*

^d *Hangzhou Institute for Advanced Study, UCAS, Hangzhou, China*

^e *School of Physics and Electronics, Henan University, Kaifeng, China*

^f *LIP6, Sorbonne Université, Paris, France*

^g *Universidad Nacional Autónoma de Honduras, Tegucigalpa, Honduras*

^h *Università di Bari, Bari, Italy*

ⁱ *Università di Bergamo, Bergamo, Italy*

^j *Università di Bologna, Bologna, Italy*

^k *Università di Cagliari, Cagliari, Italy*

^l *Università di Ferrara, Ferrara, Italy*

^m *Università di Genova, Genova, Italy*

ⁿ *Università degli Studi di Milano, Milano, Italy*

^o *Università degli Studi di Milano-Bicocca, Milano, Italy*

^p *Università di Padova, Padova, Italy*

^q *Università di Perugia, Perugia, Italy*

^r *Scuola Normale Superiore, Pisa, Italy*

^s *Università di Pisa, Pisa, Italy*

^t *Università della Basilicata, Potenza, Italy*

^u *Università di Roma Tor Vergata, Roma, Italy*

^v *Università di Siena, Siena, Italy*

^w *Università di Urbino, Urbino, Italy*

^x *Universidad de Alcalá, Alcalá de Henares, Spain*

^y *Facultad de Ciencias Físicas, Madrid, Spain*

^z *Department of Physics/Division of Particle Physics, Lund, Sweden*

[†] *Deceased*